Direct observation of the Migdal effect induced by neutron bombardment

米格达尔(Migdal)效应的直接观测

Nature **649**, 580 (2026)

刘 倩 （代表 **MARVEL** 合作组团队）

MigdAl pRocess Validation by nEutruaL scattering (中性散射中的Migdal过程验证)

中国科学院大学

2026年新物理前沿与交叉科学研讨会 南京 2026.5.16

Dark matter

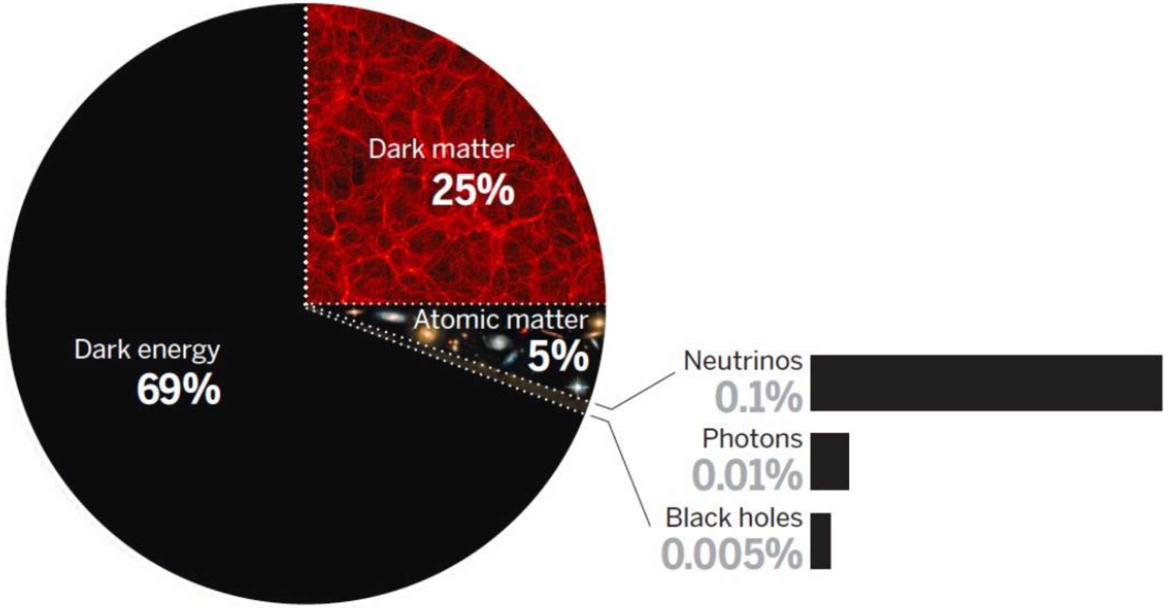

- Dark matter makes up most of the mass in galaxies and galaxy clusters.
- Current evidence comes solely from gravitational interaction.

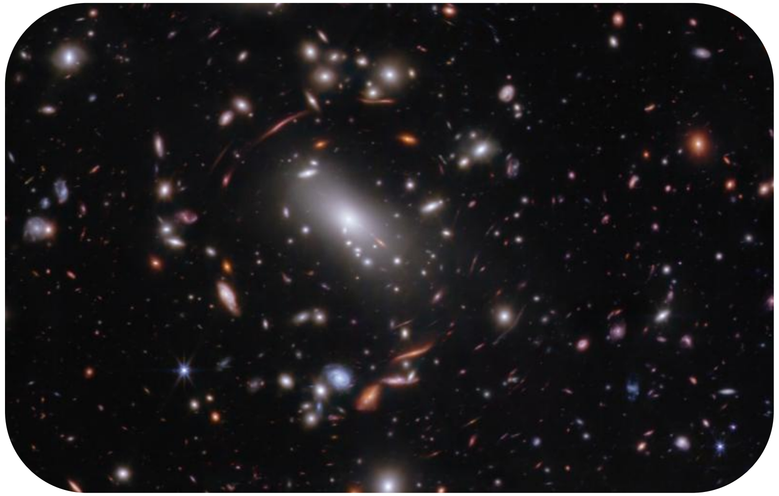

Gravitational Lens

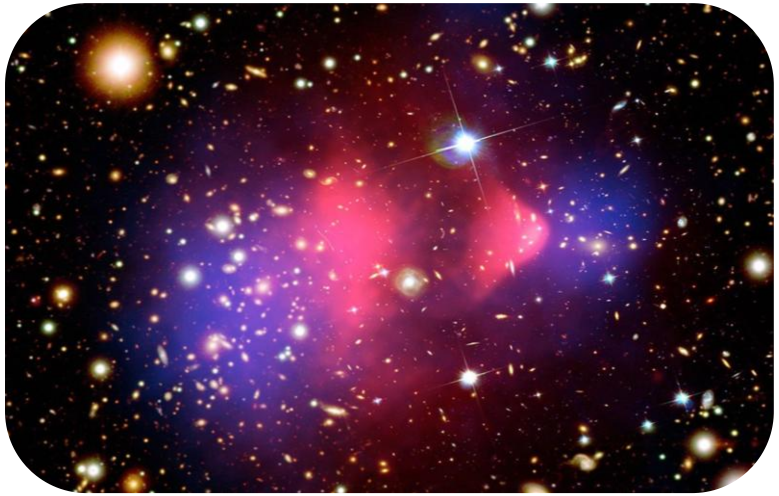

Galaxy mergers

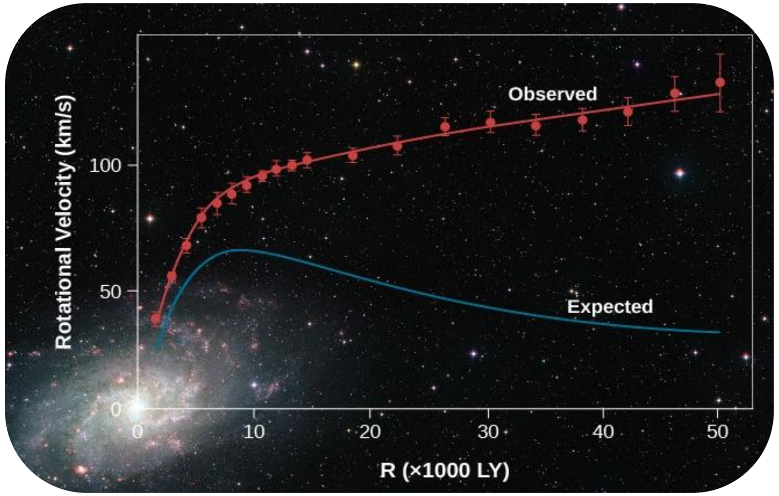

Galactic rotation curve

WIMP

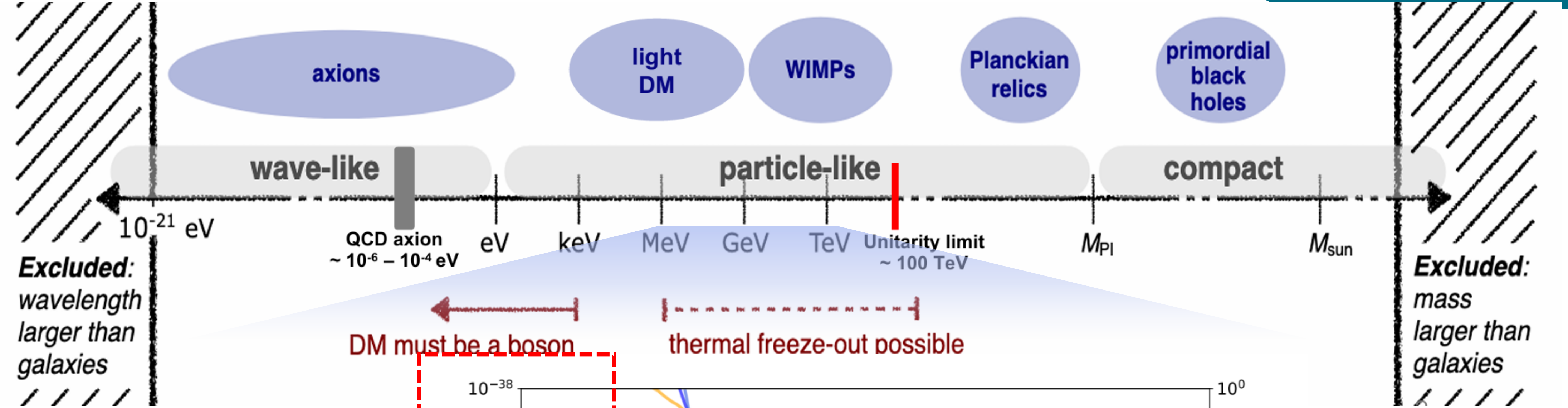

axions
light DM
WIMPs
Planckian relics
primordial black holes
wave-like
particle-like
compact
10^-21 eV
QCD axion ~ 10^-6 – 10^-4 eV
eV
keV
MeV
GeV
TeV
Unitarity limit ~ 100 TeV
M_Pl
M_sun
Excluded: wavelength larger than galaxies
Excluded: mass larger than galaxies
DM must be a boson
thermal freeze-out possible

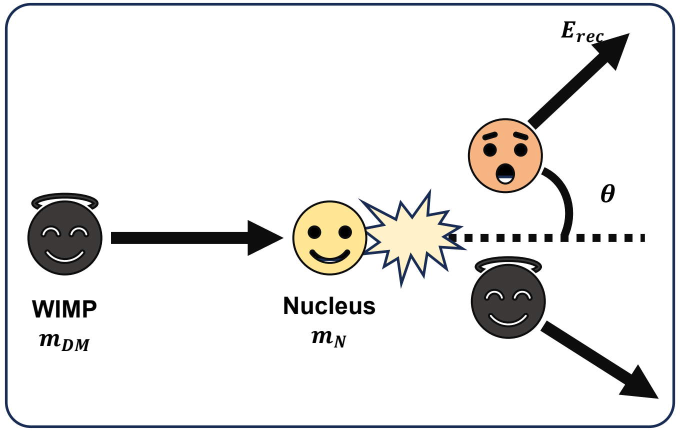

E_rec
θ
WIMP
m_DM
Nucleus
m_N

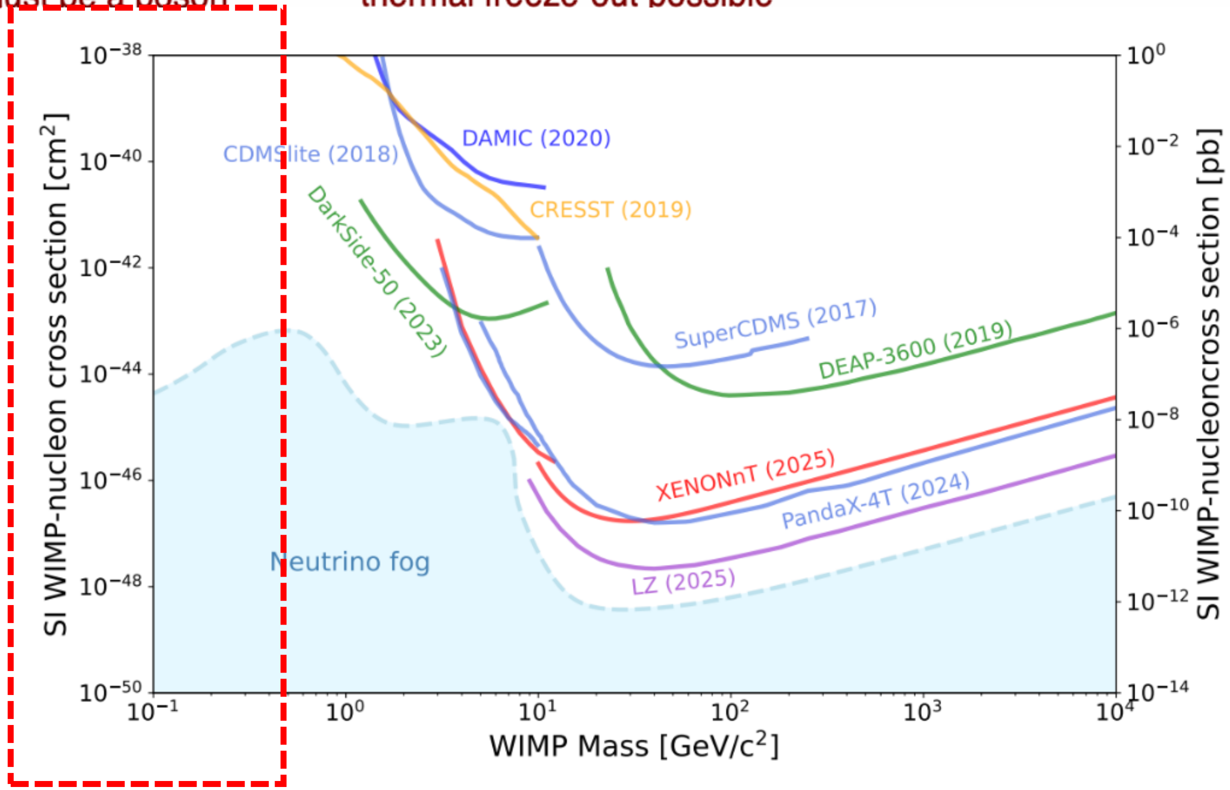

SI WIMP-nucleon cross section [cm²]
SI WIMP-nucleoncross section [pb]
WIMP Mass [GeV/c²]
DAMIC (2020)
CDMSlite (2018)
CRESST (2019)
DarkSide-50 (2023)
SuperCDMS (2017)
DEAP-3600 (2019)
XENONnT (2025)
PandaX-4T (2024)
LZ (2025)
Neutrino fog

Migdal效应

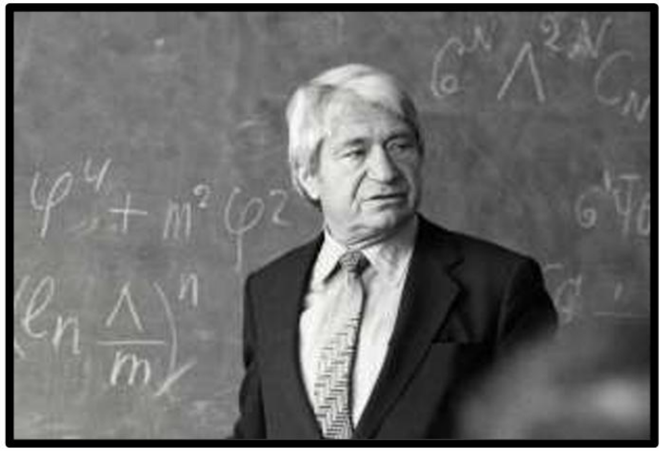

- 1939年由前苏联科学家Migdal预言

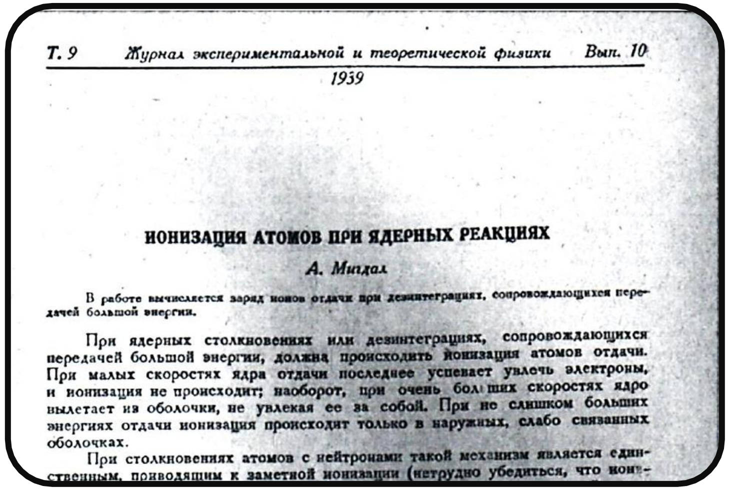

Т. 9 *Журнал экспериментальной и теоретической физики* Вып. 10

1939

ИОНИЗАЦИЯ АТОМОВ ПРИ ЯДЕРНЫХ РЕАКЦИЯХ

А. Мигдал

В работе вычисляется заряд ионов отдачи при дезинтеграциях, сопровождающихся передачей большой энергии.

При ядерных столкновениях или дезинтеграциях, сопровождающихся передачей большой энергии, должна происходить ионизация атомов отдачи. При малых скоростях ядра отдачи последнее успевает увлечь электроны, и ионизация не происходит; наоборот, при очень больших скоростях ядро вылетает из оболочки, не увлекая ее за собой. При не слишком больших энергиях отдачи ионизация происходит только в наружных, слабо связанных оболочках.

При столкновениях атомов с нейтронами такой механизм является единственным, приводящим к заметной ионизации (нетрудно убедиться, что ион-

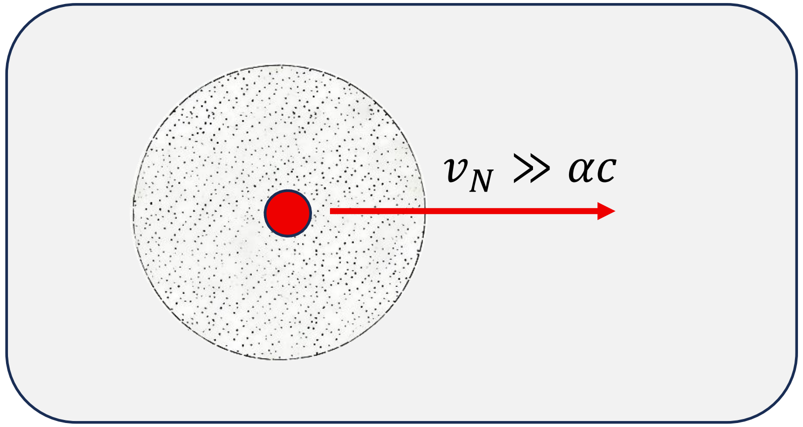

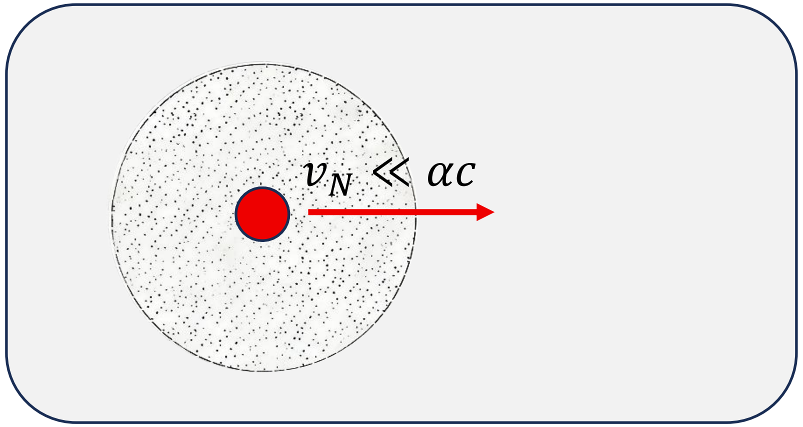

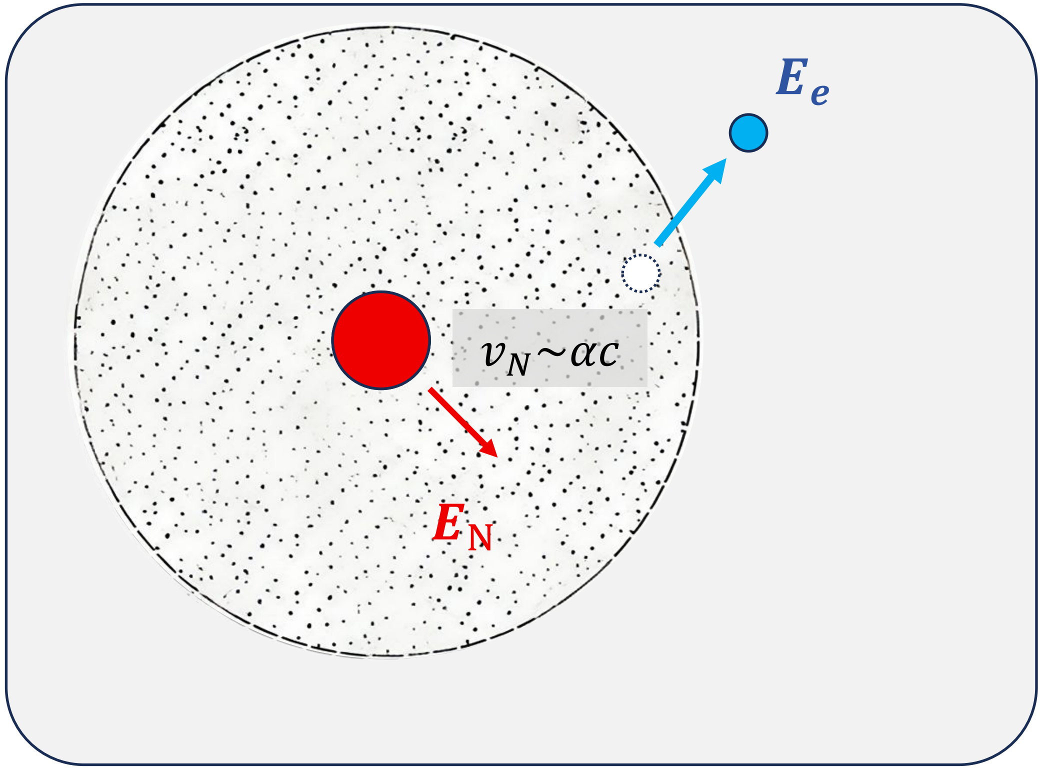

利用Migdal效应直接探测暗物质实验

$$E_{\mathrm{er,obs}} = E_{\mathrm{er}} - E_{\mathrm{bind}}$$

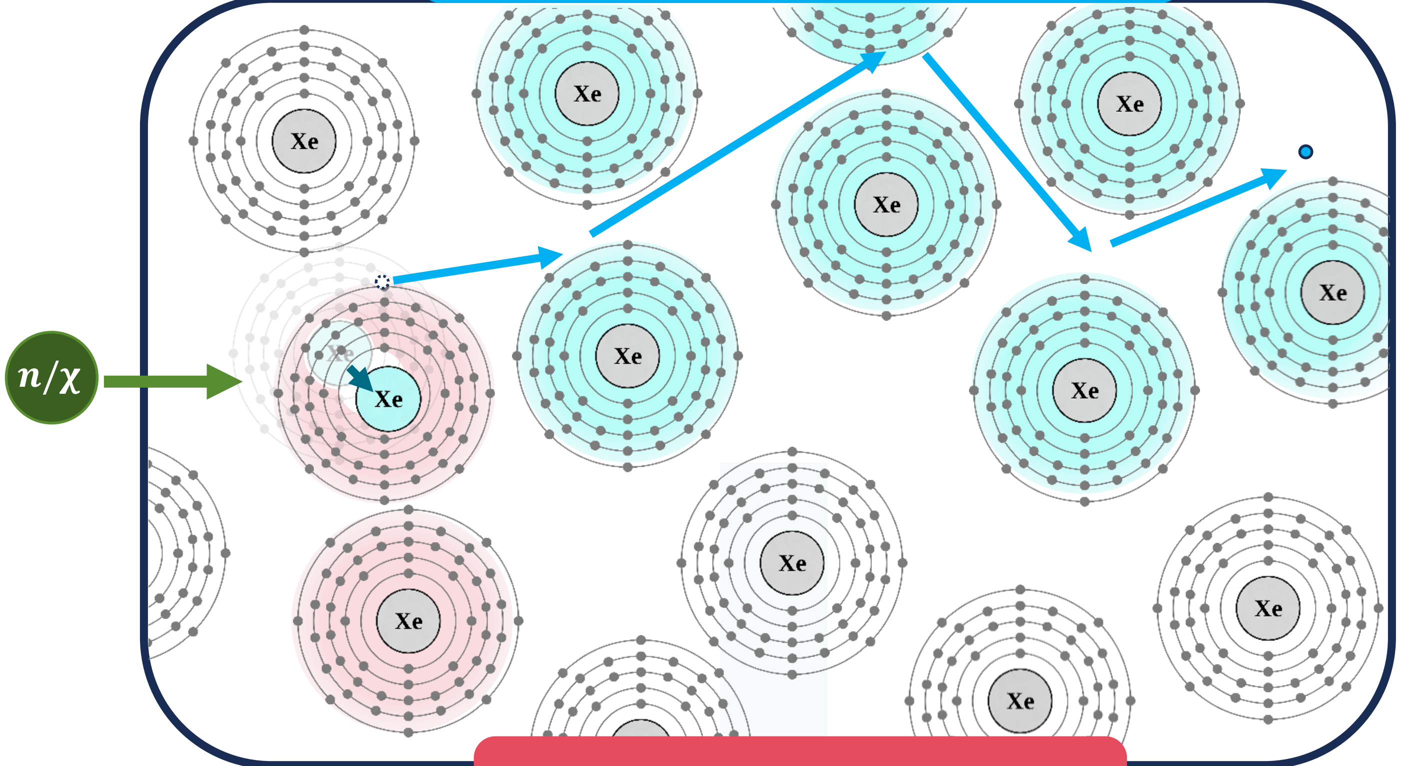

$$E_{\mathrm{nr,obs}} = E_{\mathrm{nr}} \cdot \varepsilon_{\mathrm{QF}}$$

$$E_{\mathrm{det}} = E_{\mathrm{er,obs}} + E_{\mathrm{nr,obs}} + \ldots$$

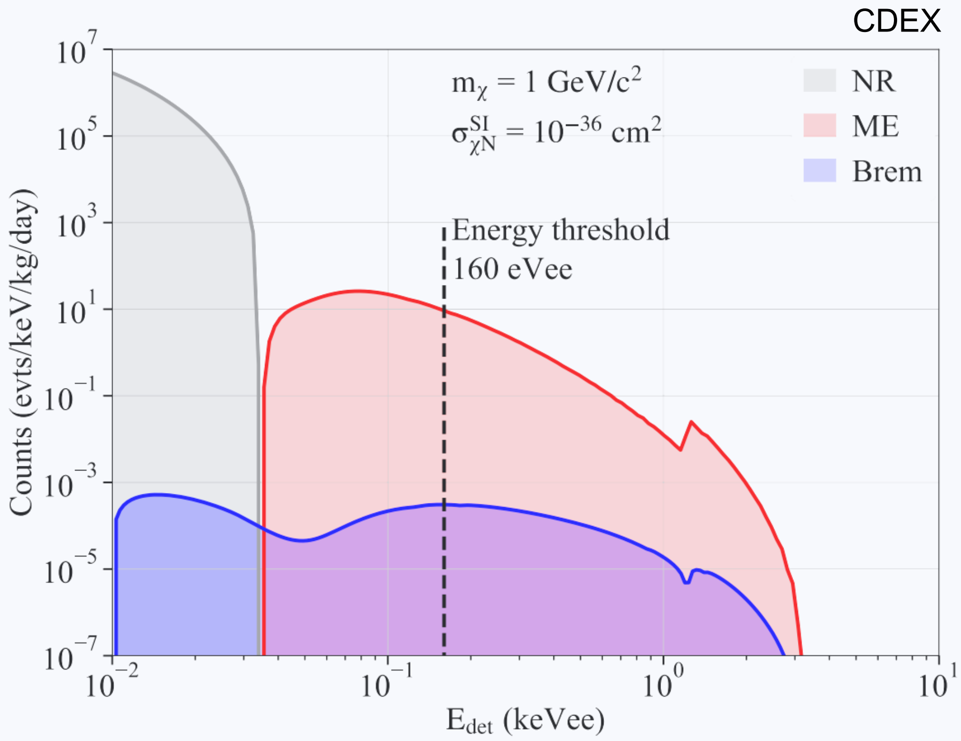

在低动量转移情况下仍然提供可探测信号！

中性粒子碰撞中的Migdal效应

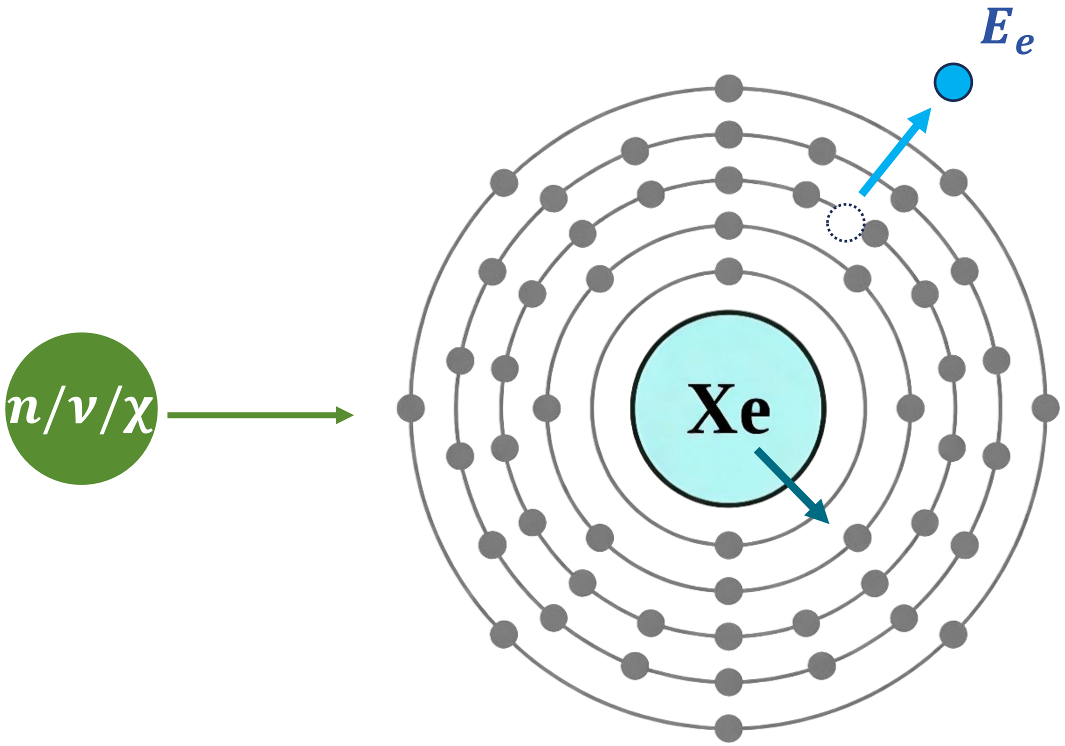

至今已有80余年，仍未有直接观测的证据

轻质量暗物质区间的探测限—由Migdal效应主导

MARVEL

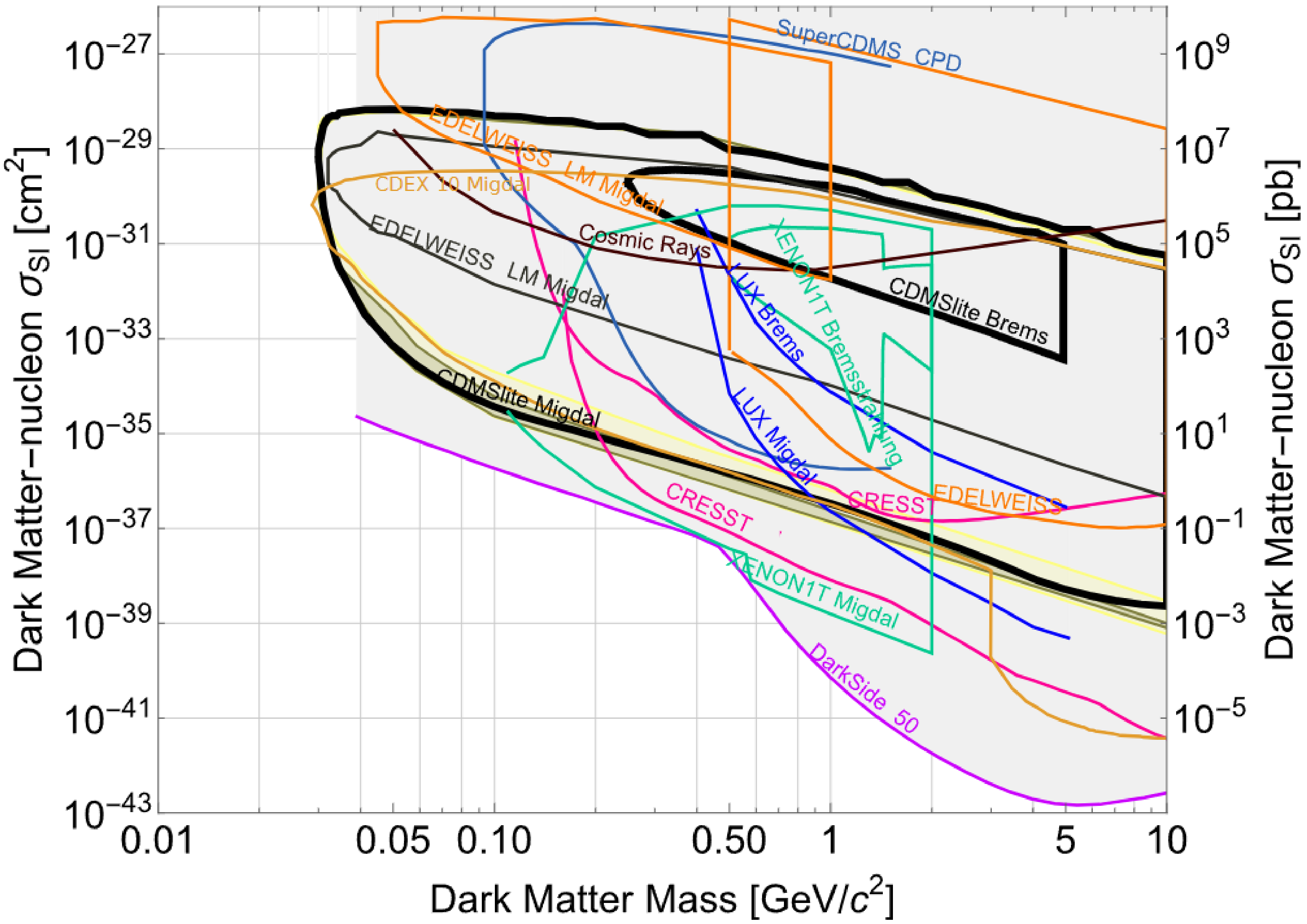

Search for Light Dark Matter Interactions Enhanced by the Migdal Effect or Bremsstrahlung in XENON1T #1
XENON Collaboration • E. Aprile (Columbia U.) et al. (Jul 30, 2019)
Published in: *Phys.Rev.Lett.* 123 (2019) 24, 241803 • e-Print: 1907.12771 [hep-ex]
pdf DOI cite claim reference search 329 citations

Search for new physics in low-energy electron recoils from the first LZ exposure #1
LZ Collaboration • J. Aalbers (SLAC and Stanford U., Phys. Dept. and KIPAC, Menlo Park) et al. (Jul 28, 2023)
Published in: *Phys.Rev.D* 108 (2023) 7, 072006 • e-Print: 2307.15753 [hep-ex]
pdf links DOI cite datasets claim reference search 73 citations

Search for Dark-Matter–Nucleon Interactions with a Dark Mediator in PandaX-4T #1
PandaX Collaboration • Di Huang (Shanghai Jiao Tong U.) et al. (Aug 3, 2023)
Published in: *Phys.Rev.Lett.* 131 (2023) 19, 191002 • e-Print: 2308.01540 [hep-ex]
pdf DOI cite claim reference search 51 citations

Results of a Search for Sub-GeV Dark Matter Using 2013 LUX Data #1
LUX Collaboration • D.S. Akerib (Case Western Reserve U. and SLAC and KIPAC, Menlo Park) et al. (Nov 27, 2018)
Published in: *Phys.Rev.Lett.* 122 (2019) 13, 131301 • e-Print: 1811.11241 [astro-ph.CO]
pdf DOI cite claim reference search 213 citations

Search for Dark-Matter–Nucleon Interactions via Migdal Effect with DarkSide-50 #1
DarkSide Collaboration • P. Agnes (Royal Holloway, U. of London) et al. (Jul 25, 2022)
Published in: *Phys.Rev.Lett.* 130 (2023) 10, 10 • e-Print: 2207.11967 [hep-ex]
pdf links DOI cite claim reference search 107 citations

Search for low-mass dark matter via bremsstrahlung radiation and the Migdal effect in SuperCDMS #1
SuperCDMS Collaboration • M.F. Albakry (British Columbia U. and TRIUMF) et al. (Feb 17, 2023)
Published in: *Phys.Rev.D* 107 (2023) 11, 2023 • e-Print: 2302.09115 [hep-ex]
pdf links DOI cite claim reference search 43 citations

Search for sub-GeV dark matter via the Migdal effect with an EDELWEISS germanium detector with NbSi transition-edge sensors #2
EDELWEISS Collaboration • E. Armengaud (IRFU, Saclay) et al. (Mar 8, 2022)
Published in: *Phys.Rev.D* 106 (2022) 6, 062004 • e-Print: 2203.03993 [astro-ph.GA]
pdf DOI cite claim reference search 66 citations

各大暗物质实验：
XENON/LZ/PandaX/CDEX/DarkSide50/
SuperCDMS/EDELWEISS/LUX…

国际上中性粒子Migdal效应实验

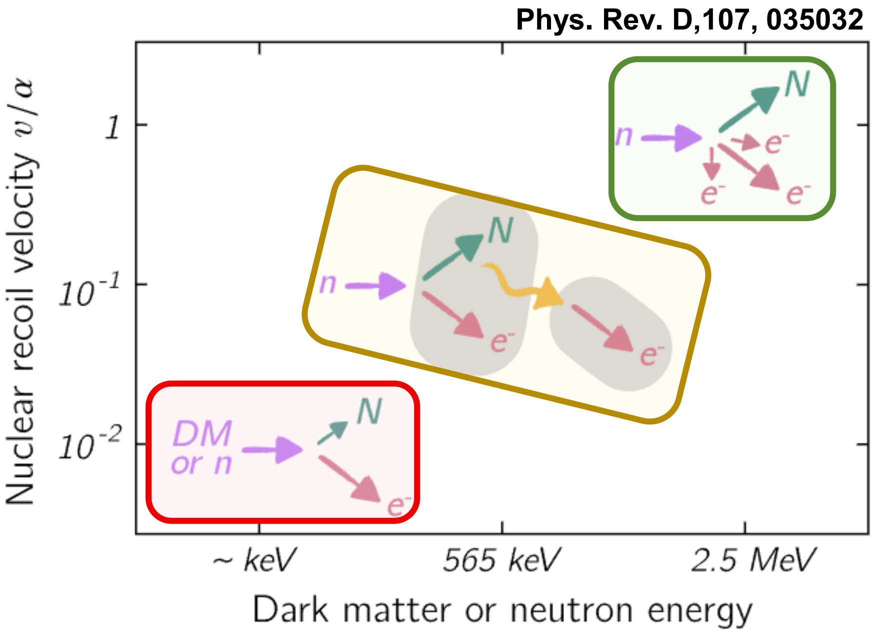

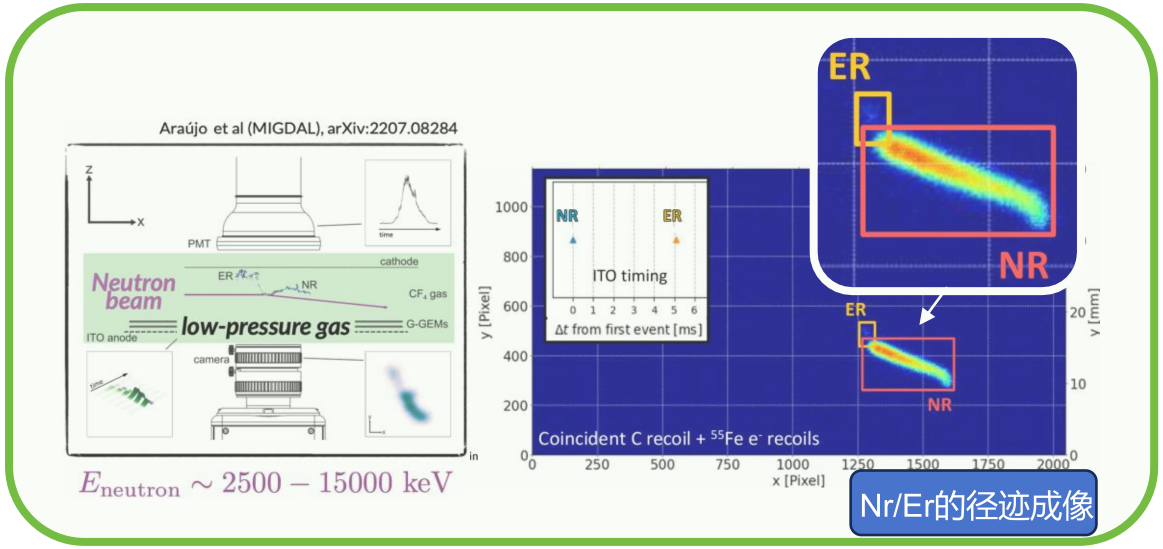

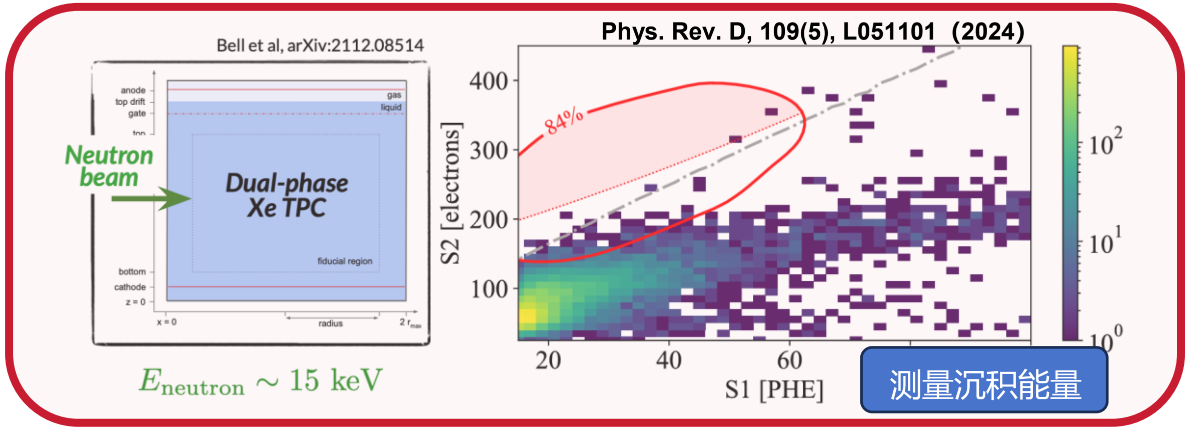

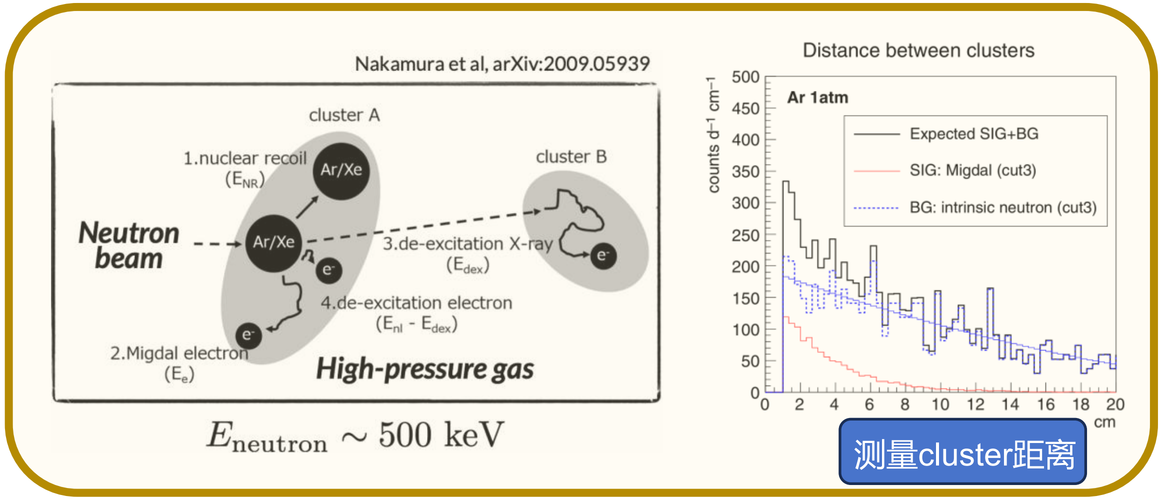

Detector Requirements

ER: 5.9 keV , NR: 300 keV

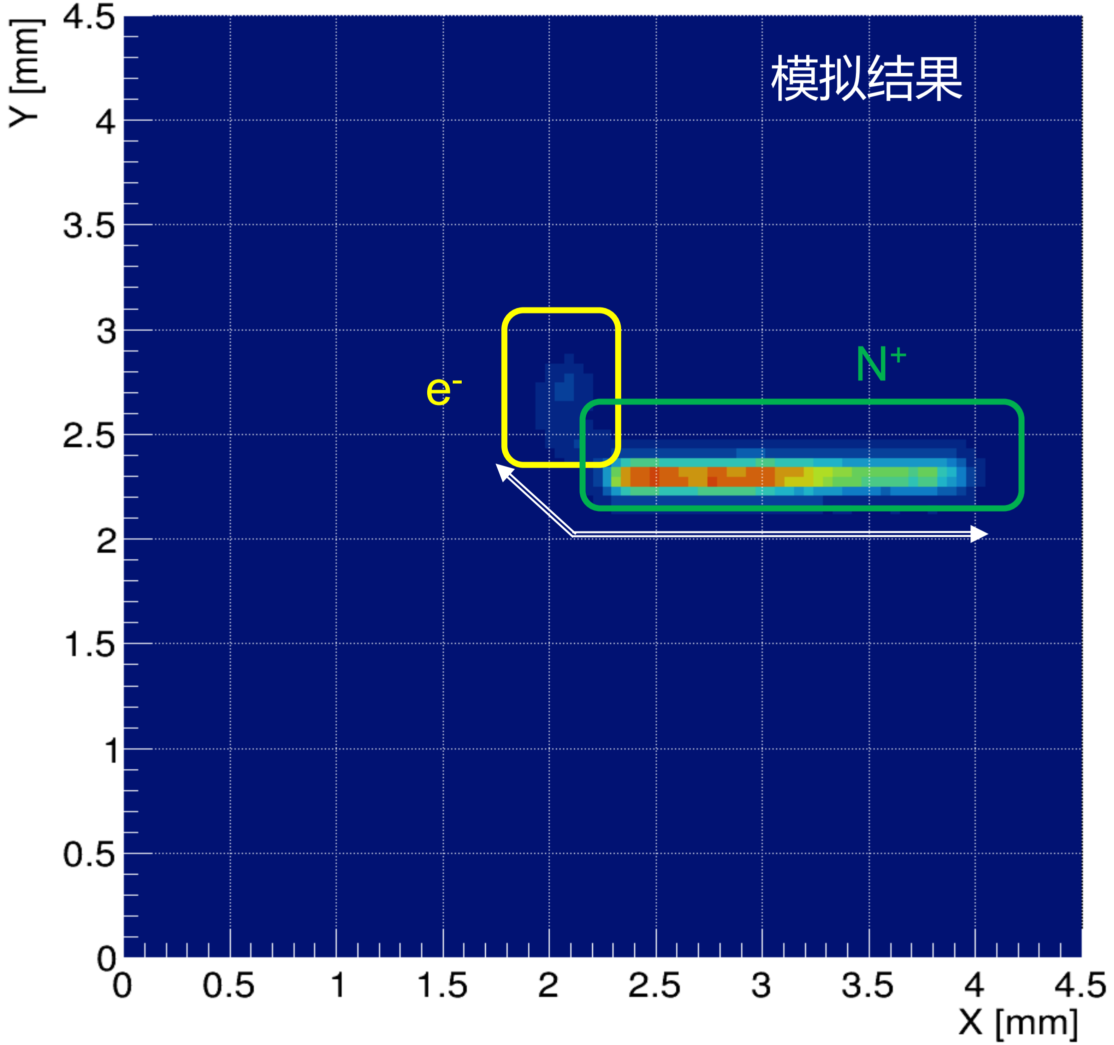

- **ER~keV，NR~hundreds keV**
  - Good energy resolution
  - Large dynamic range.
- **ER shares vertex with NR**
  - Good vertex resolution
- **Reduce possible background**
  - Good time resolution

MARVEL 实验装置示意

GMCP

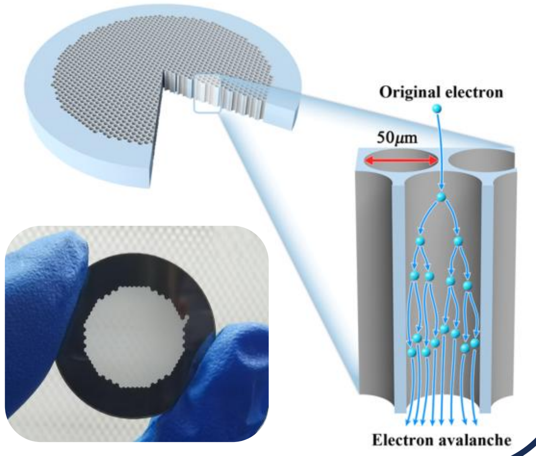

Topmetal-II

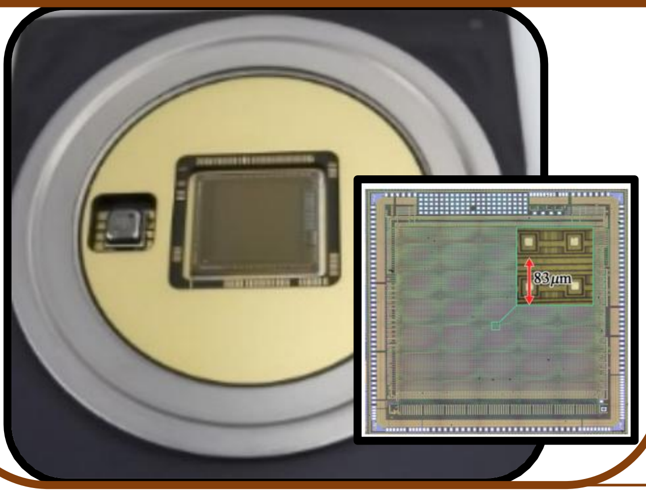

提出全新的实验手段

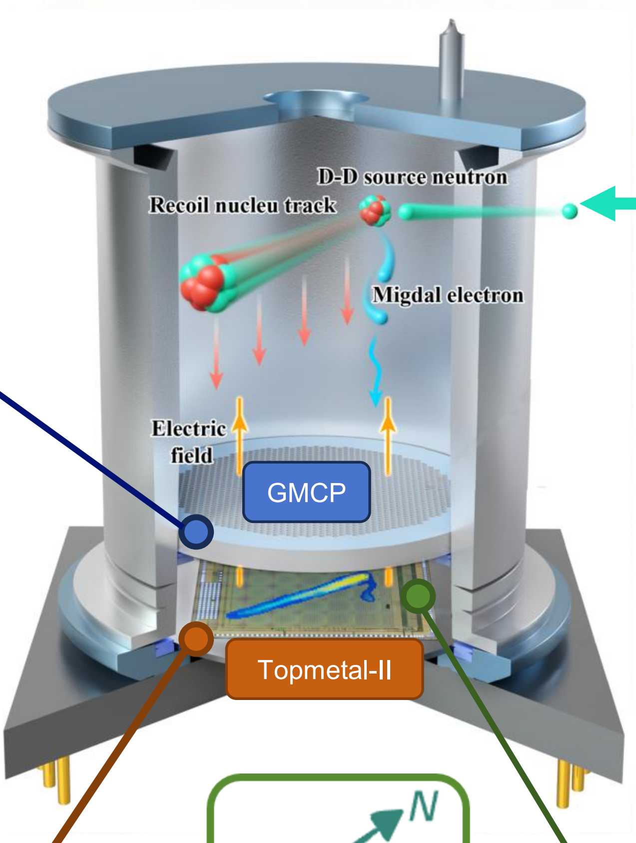

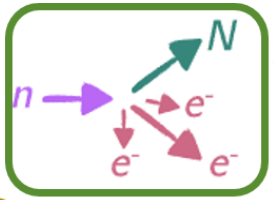

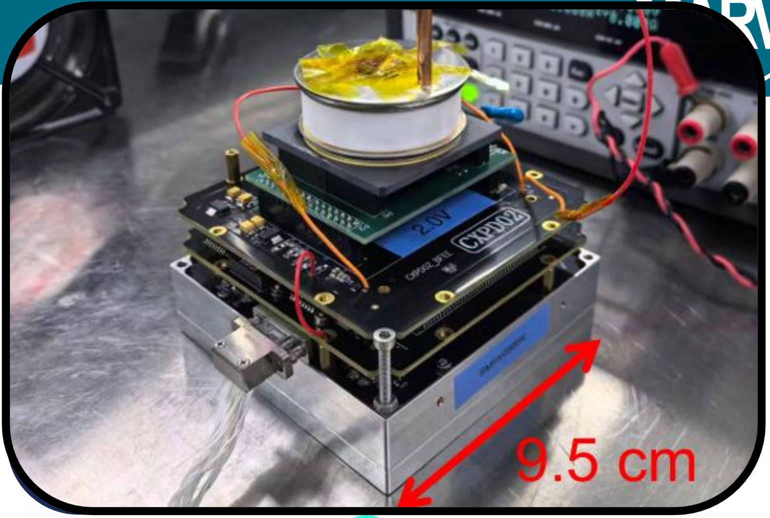

DD neutron source

Migdal topology

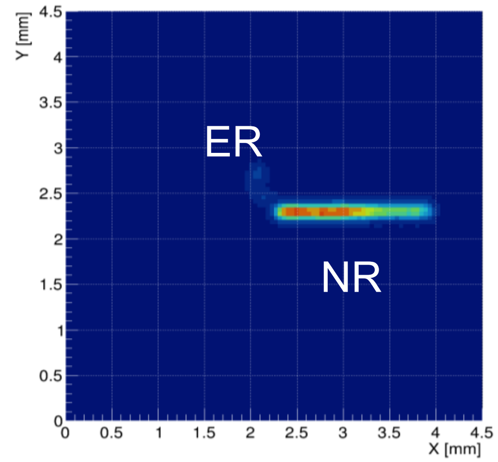

核心器件：GMCP

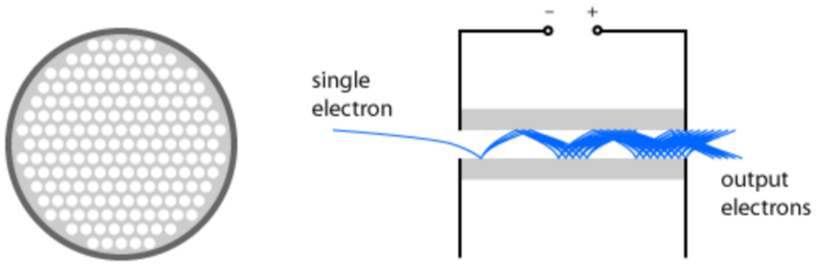

真空器件微通道板（MCP）

刘宏邦

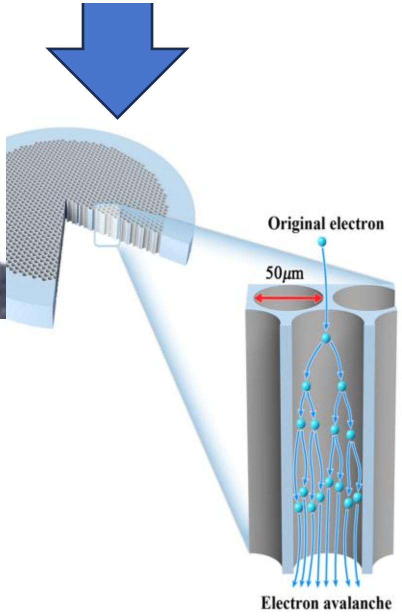

运用于气体探测器（GMCP）

- 微结构气体探测器：GEM/THGEM、MicroMegas…
- 真空器件MCP并不能直接在气体下使用！
- 电荷累积在GEM孔内导致增益下降！
- 设计新工艺，在孔内制作阻性材料，释放电荷

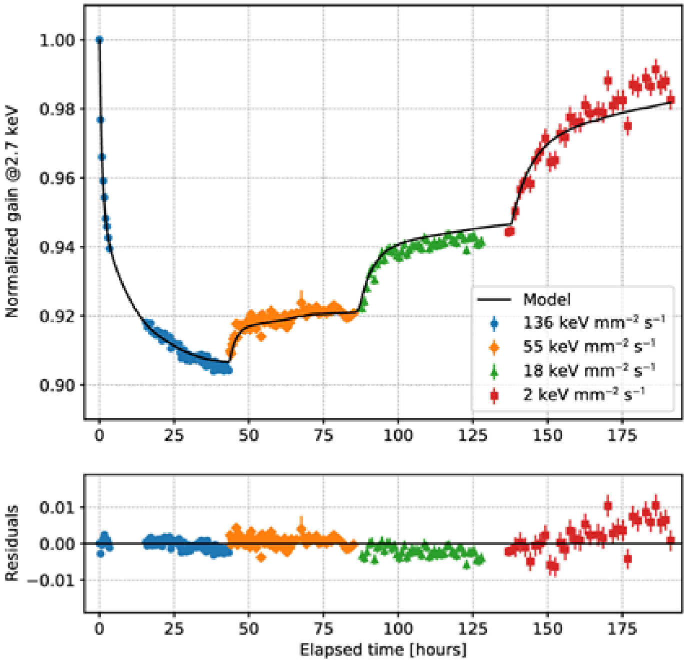

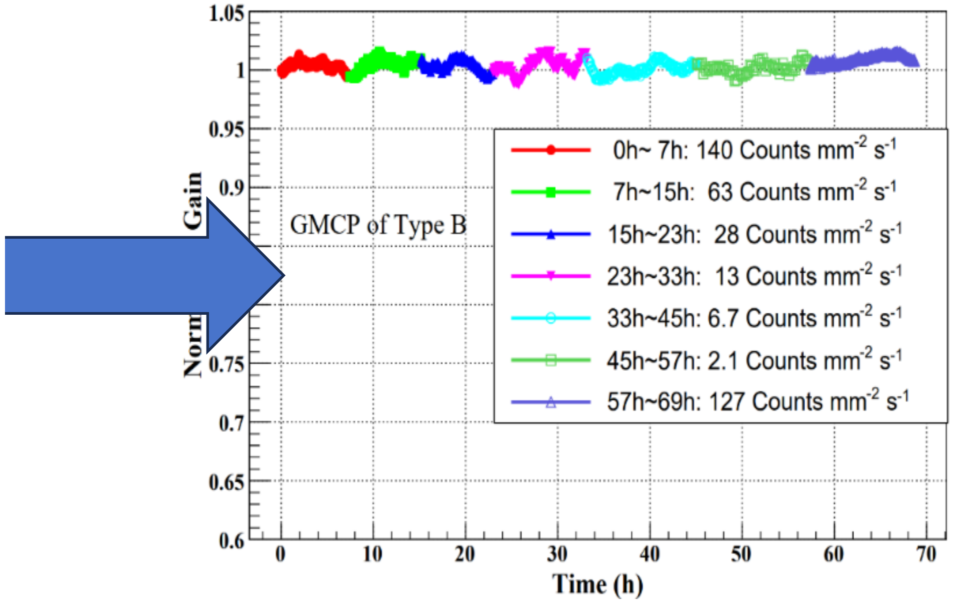

核心器件：像素芯片Topmetal

MARVEL

孙向明

Topmetal-II

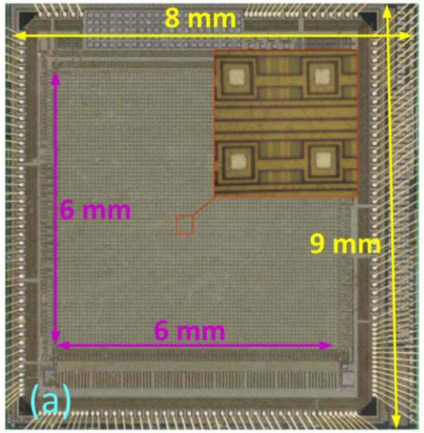

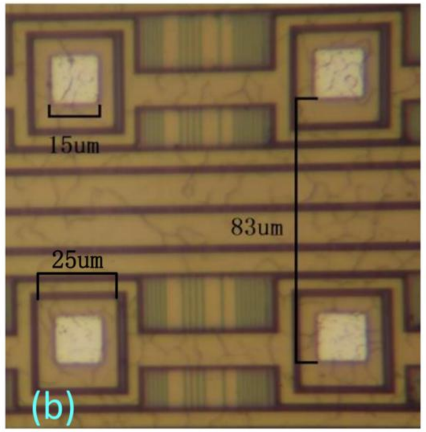

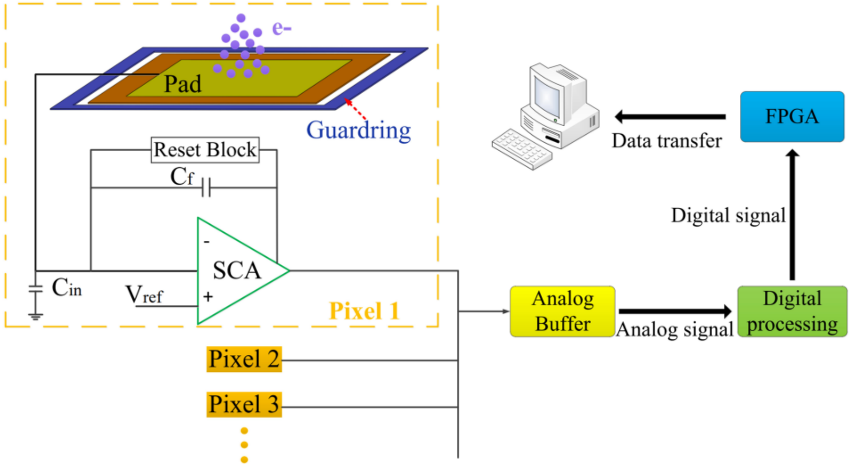

	Topmetal-II$^-$	Topmetal-M1/M2	Topmetal-L
Chip Size /mm^2	6 × 6	18 × 23	17 × 24
Pixel Array	72 × 72	400 × 512	356 × 512
Pixel Size /um^2	83 × 83	45 × 45	45 × 45
ENC	~ 13.4e-	~ 15.4e-	~ 20.0e-
Power Consumption	~ 1W @3.3V	~ 4.3W @3.3V	**~ 0.8W @3.3V**
Clock	40MHz	5MHz	20MHz
Frame Rate	2.5ms	2.4ms	0.37ms @Sentinel Readout
Readout Mode	Rolling Shutter	Rolling Shutter	Rolling Shutter **/Sentinel Readout**
Readout Channel	1	16	1

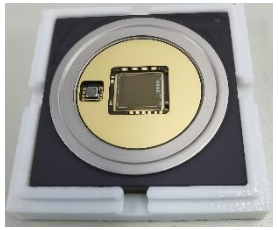

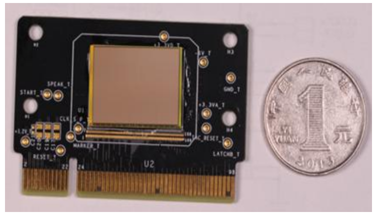

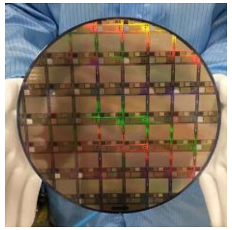

Detector performance

Energy resolution

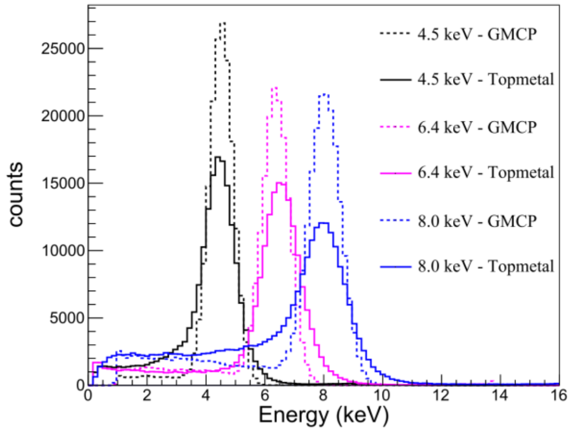

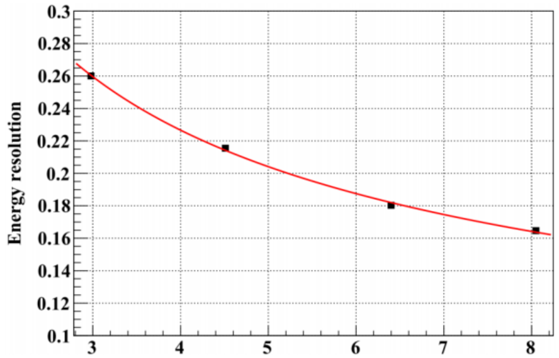

- Good linear energy response
- 20%-30% energy resolution(FWHM)
- Energy resolution follows the relationship ~ $1/\sqrt{E}$

Dynamic range

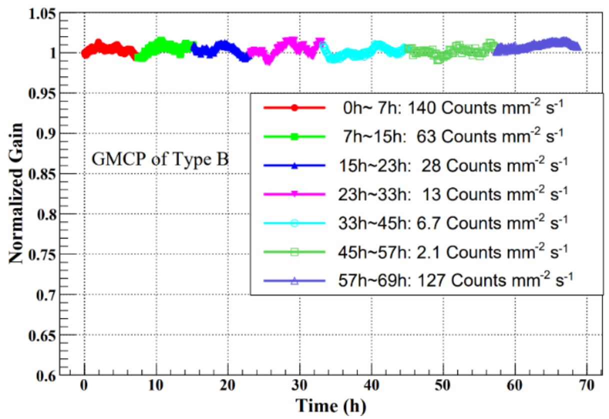

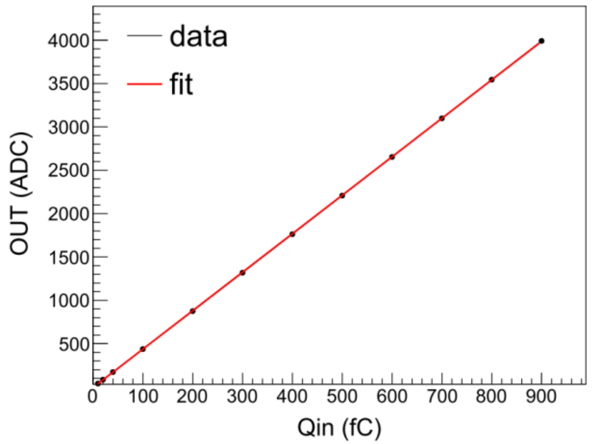

- Stable gain under different count rates(no pile up)
- Good linearity in charge response

Vertex resolution

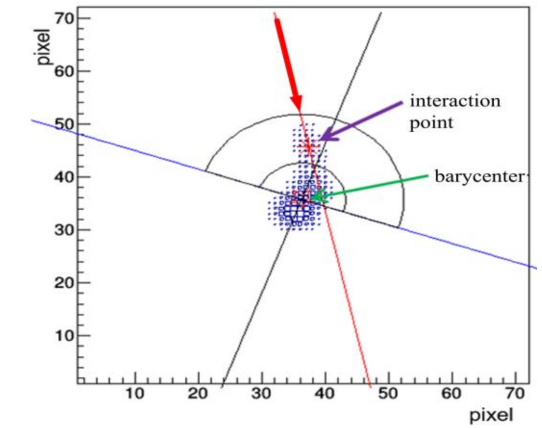

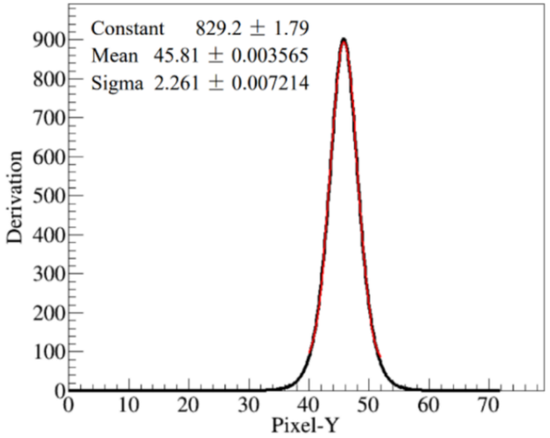

- ~200 μm vertex resolution @ 6.4 keV

Time resolution

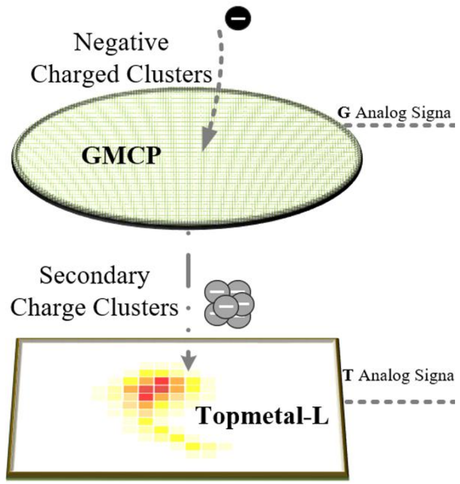

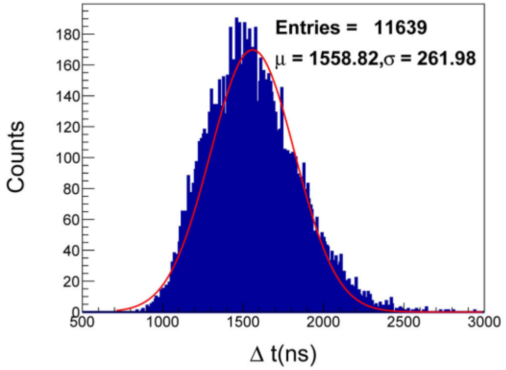

- ~262 ns time resolution

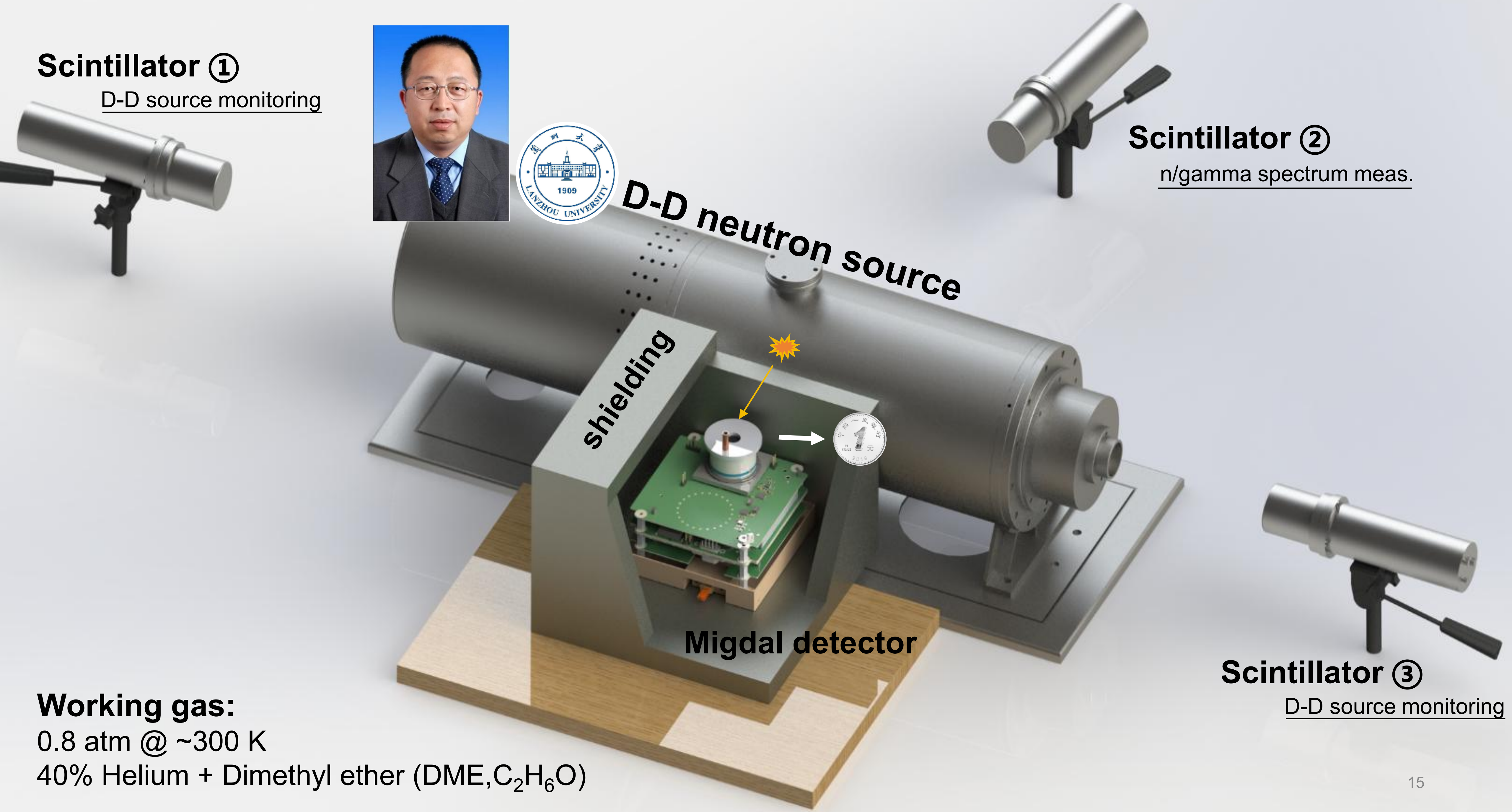

Working gas:

0.8 atm @ ~300 K

40% Helium + Dimethyl ether (DME,C_2H_6O)

事例挑选

Data → YOLO*[1] preselection → NR reconstruction → ER reconstruction → Vertex cut

YOLOv8.2

Labeling

Dataset		Train	Valid
Exp	^{55}Fe	3000	1493
	D-D	2994	1354
Sim	ER	1200	301
	NR	1200	301
Total		8394	3449

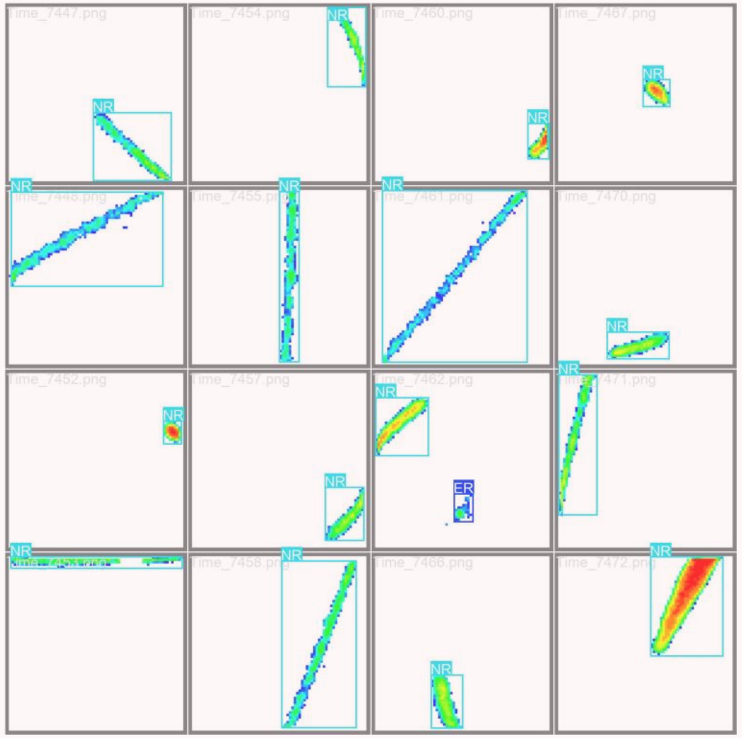

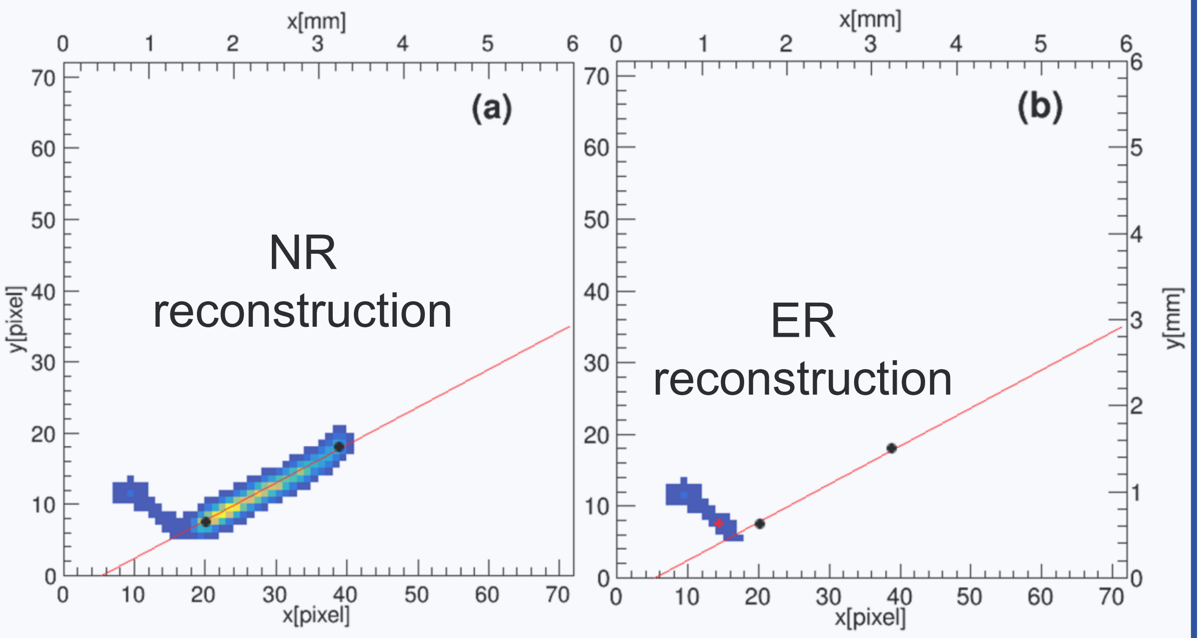

Migdal 事例

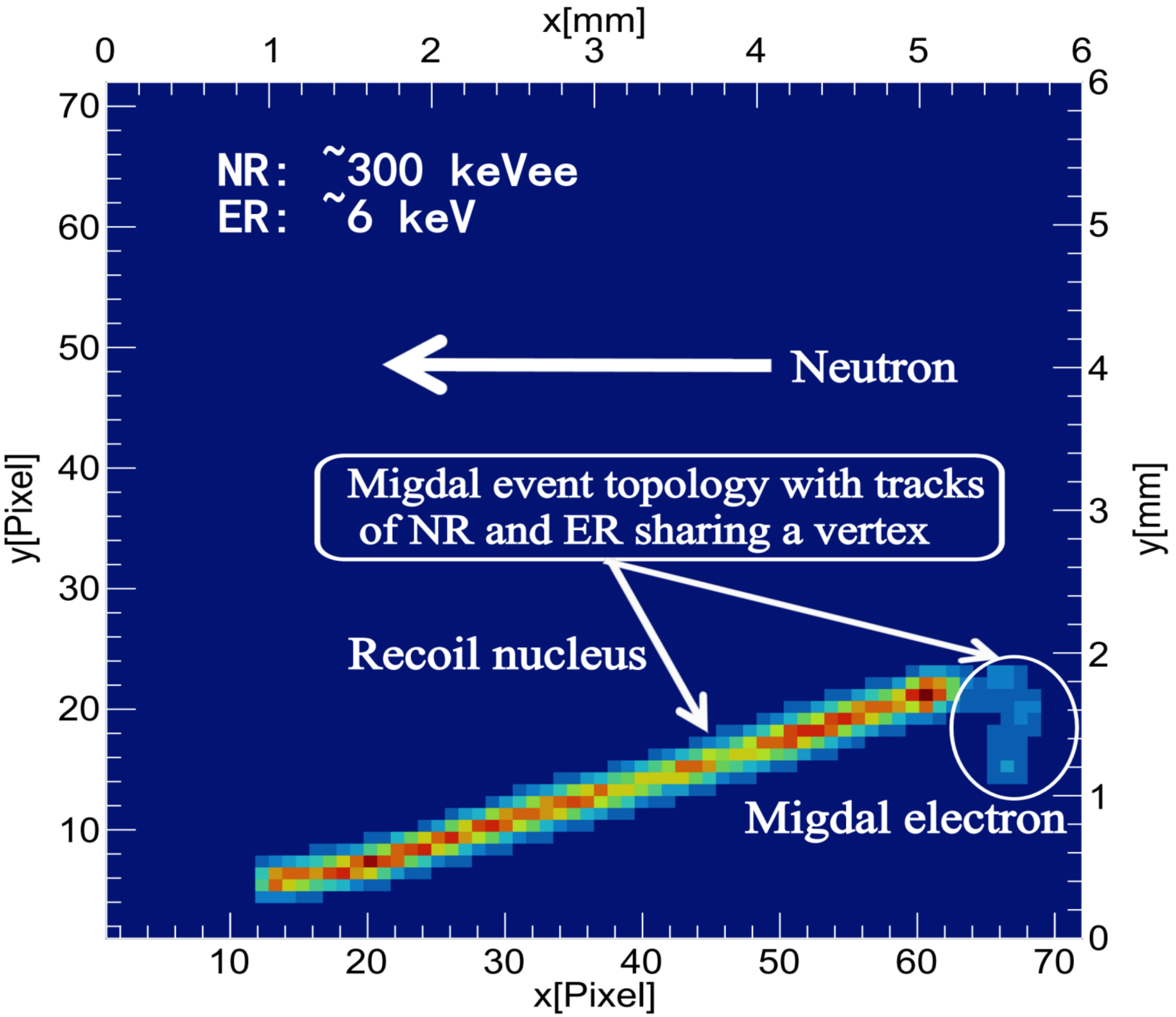

x[mm]
0
1
2
3
4
5
6
70
60
50
40
30
20
10
y[Pixel]
6
5
4
3
2
1
0
y[mm]
NR: ~300 keVee
ER: ~6 keV
Neutron
Migdal event topology with tracks of NR and ER sharing a vertex
Recoil nucleus
Migdal electron
10
20
30
40
50
60
70
x[Pixel]

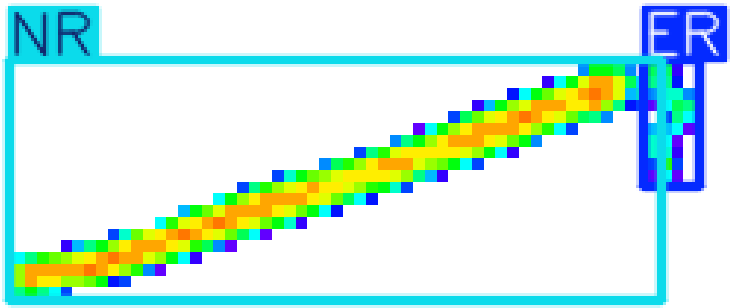

NR
ER

更多的Migdal事例！

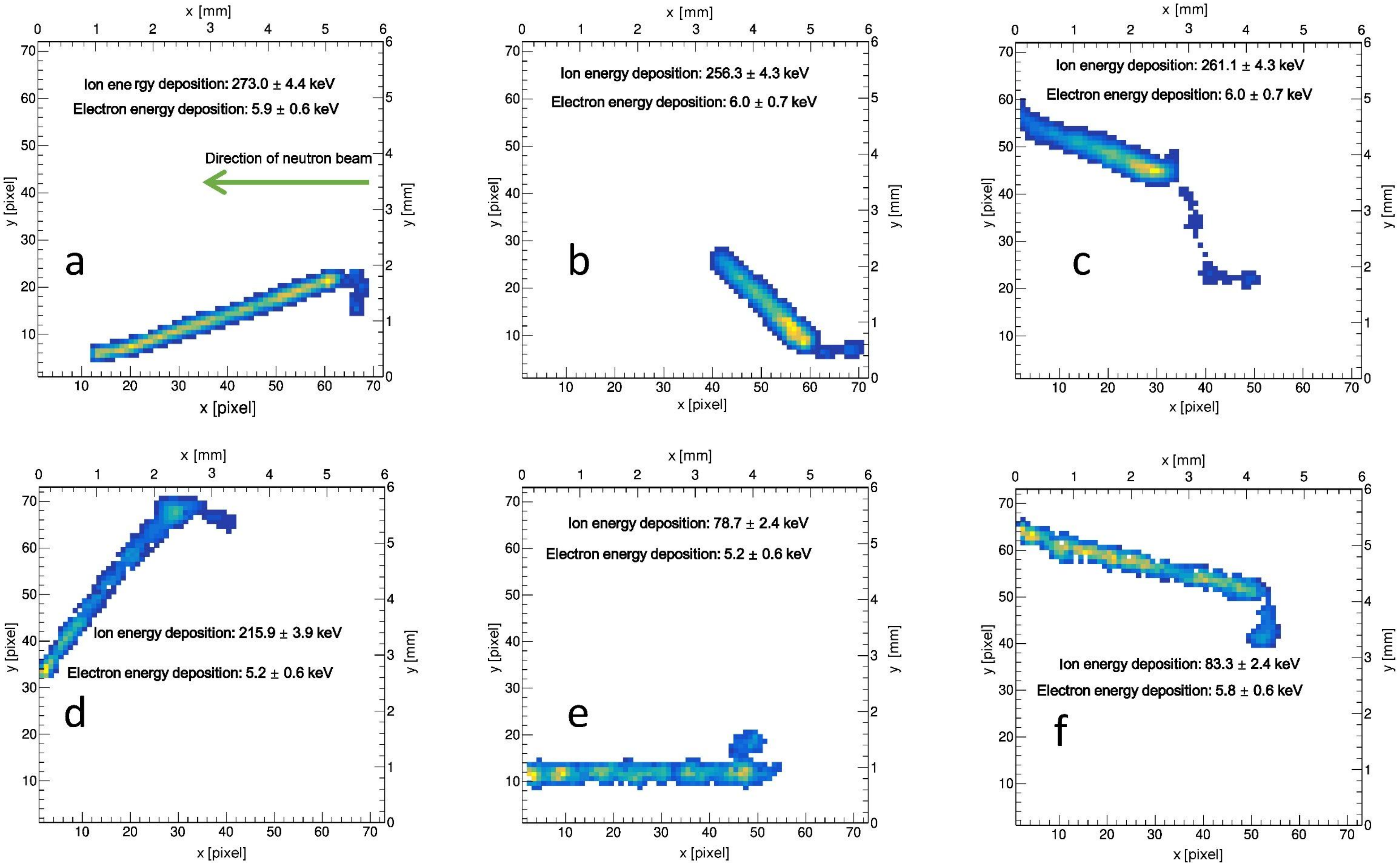

全部通过YOLO识别！

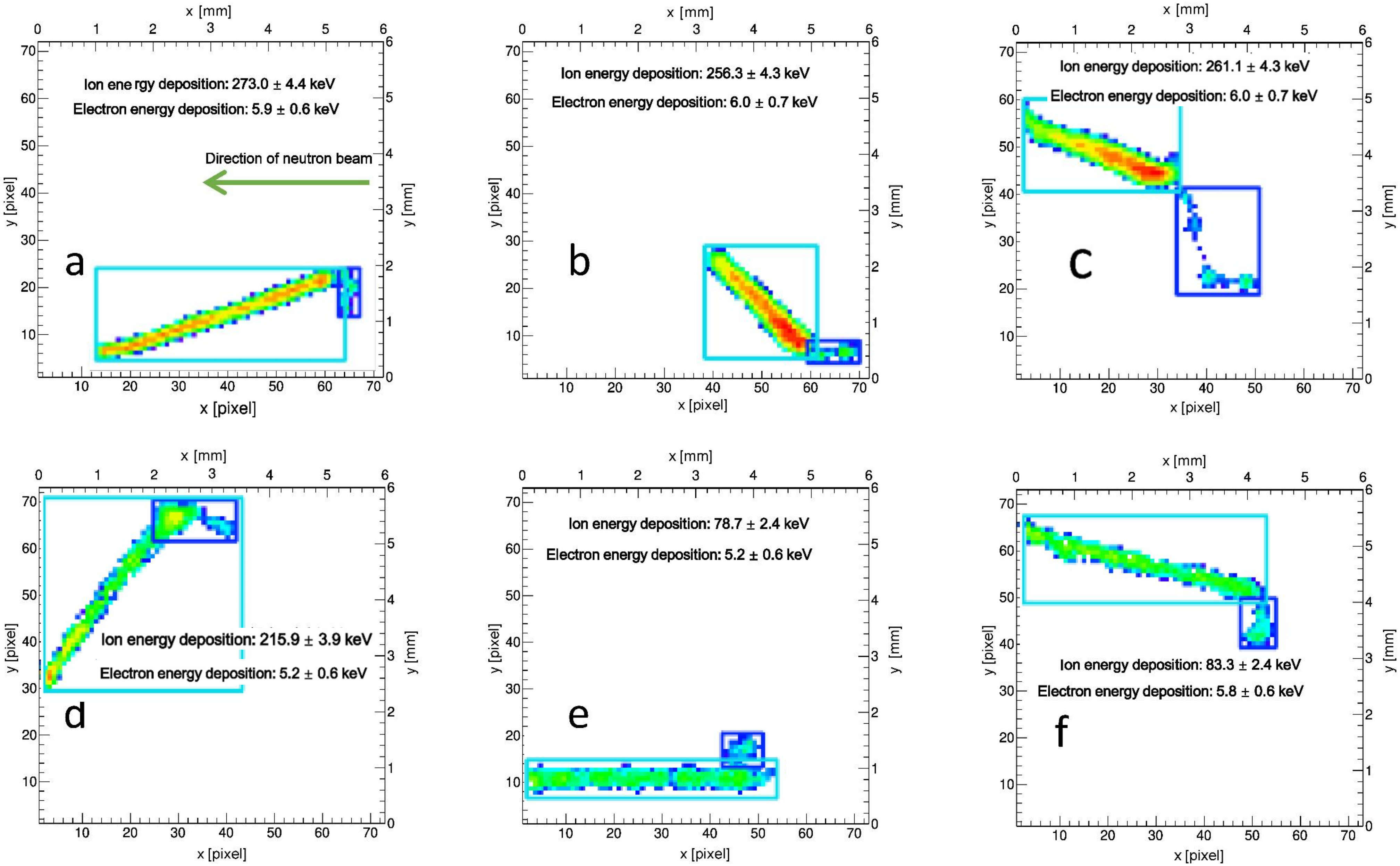

a
Ion ene rgy deposition: 273.0 ± 4.4 keV
Electron energy deposition: 5.9 ± 0.6 keV
Direction of neutron beam
b
Ion energy deposition: 256.3 ± 4.3 keV
Electron energy deposition: 6.0 ± 0.7 keV
c
Ion energy deposition: 261.1 ± 4.3 keV
Electron energy deposition: 6.0 ± 0.7 keV
d
Ion energy deposition: 215.9 ± 3.9 keV
Electron energy deposition: 5.2 ± 0.6 keV
e
Ion energy deposition: 78.7 ± 2.4 keV
Electron energy deposition: 5.2 ± 0.6 keV
f
Ion energy deposition: 83.3 ± 2.4 keV
Electron energy deposition: 5.8 ± 0.6 keV
x [mm]
x [pixel]
y [pixel]
y [mm]

电子与核子径迹

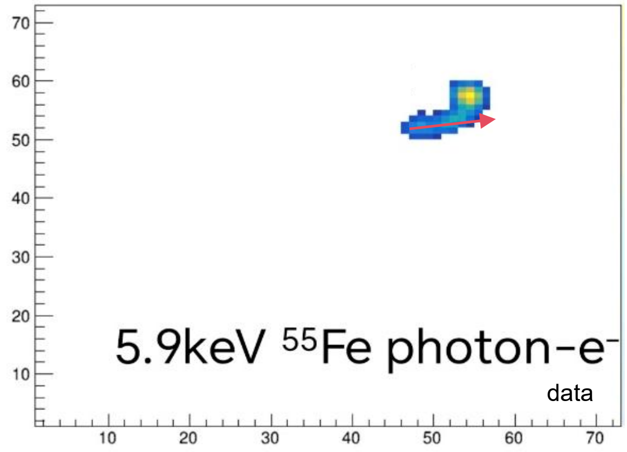

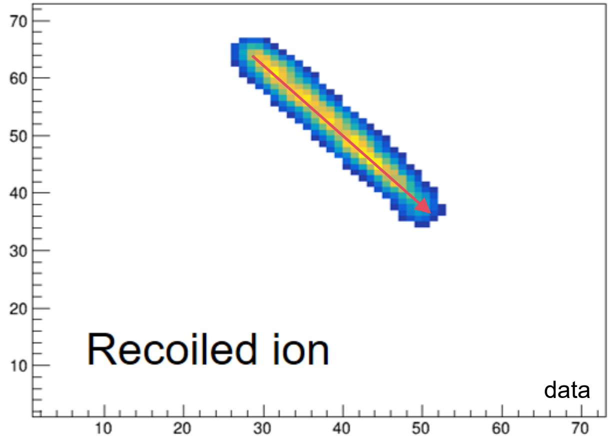

$5\ keV_{ee} < Ee < 10\ keV_{ee}, E_{nr} > 35keV_{ee}$

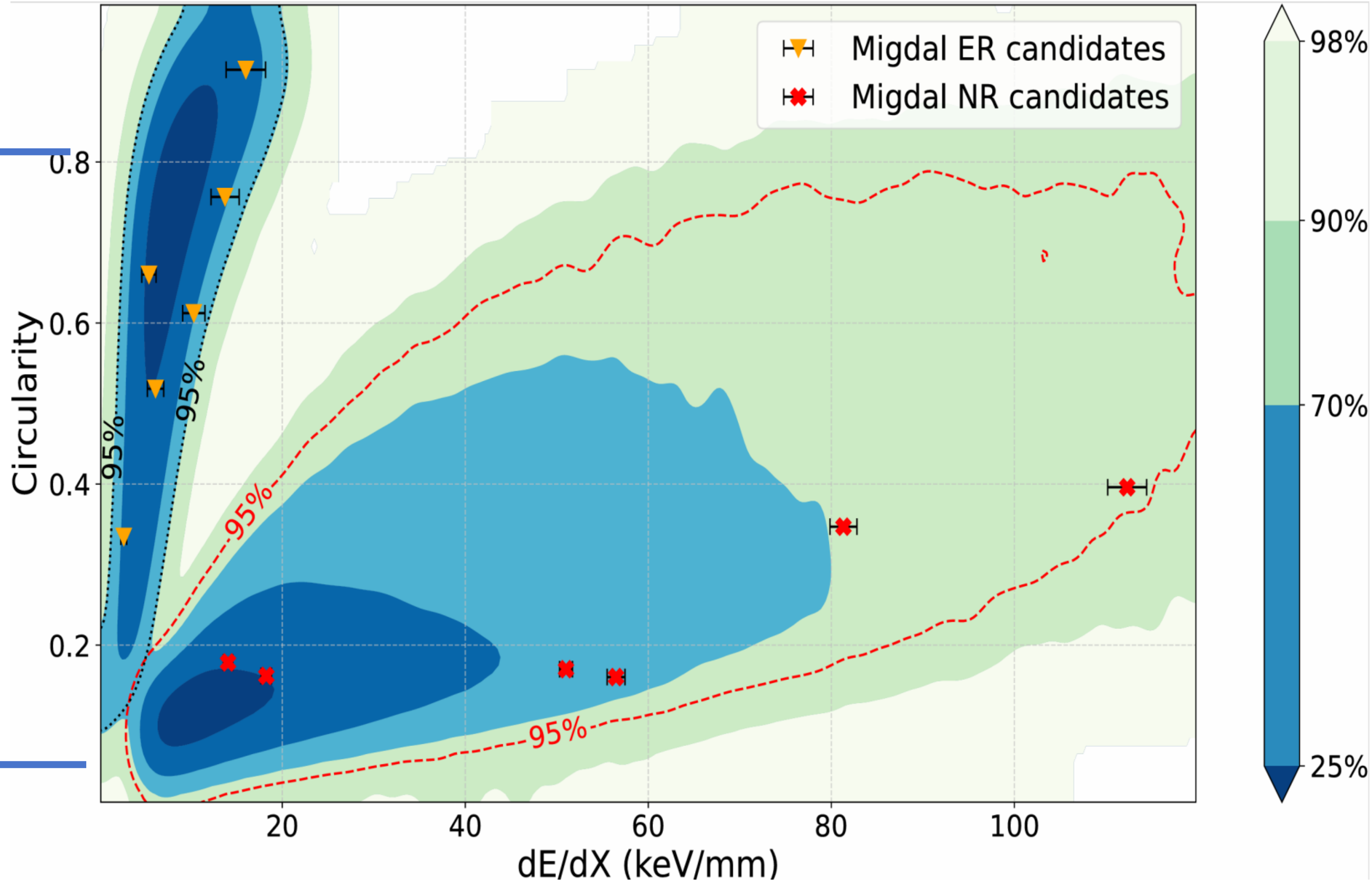

Migdal事例中的电子与^{55}Fe源的光电子样本区间一致；核反冲径迹与中子数据中核反冲控制样本一致！

本底估计

Background Component	Description	Expectation value (5 - 10 keV)	Method
Recoil induced δ ray	δ electron near NR track origin	0.035±0.023(stat.)±0.0068(sys.)	Data driven
Particle Induced X-ray Emission			
X-ray emission	Photoelectron near NR track origin	0	
Auger electrons	Auger electron near NR track origin	0	
Bremsstrahlung processes			
Quasi-Free Electron (QFEB)	Photoelectron near NR track origin	≈ 0	
Secondary Electron (SEB)	Photoelectron near NR track origin	≈ 0	
Atomic (AB)	Photoelectron near NR track origin	≈ 0	
Nuclear (NB)	Photoelectron near NR track origin	≈ 0	
Random track coincidences	Photo-/Compton electron near NR track	0.180±0.022(stat.)±0.042(sys.)	Data driven
Muon induced δ ray	δ electron near NR track origin	0.013	MC+Data
Gas radioactivity			
Trace contaminants	Electron from decay near NR track origin	0.001±0.00087(sys.)	Data driven
Neutron activation	Electron from decay near NR track origin	≈ 0	
Secondary nuclear recoil fork	NR track fork near track origin	≈ 0	
Total background		0.229±0.032(stat.)±0.043(sys.)	

武雷 祝斌

1. Delta电子本底

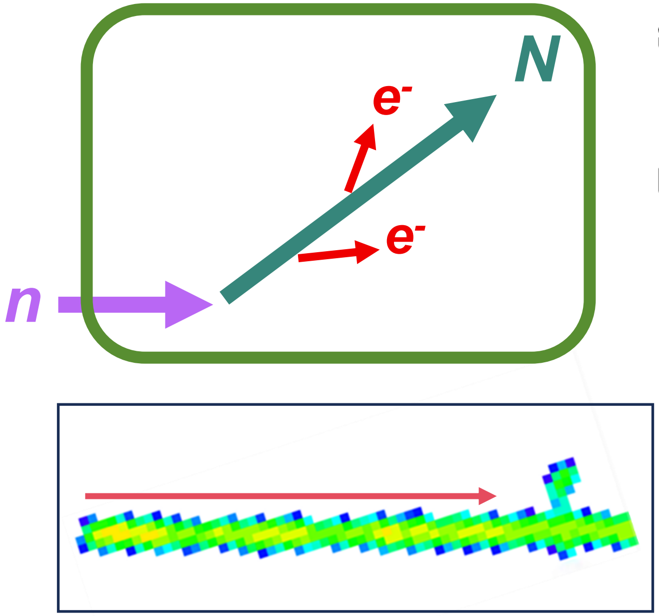

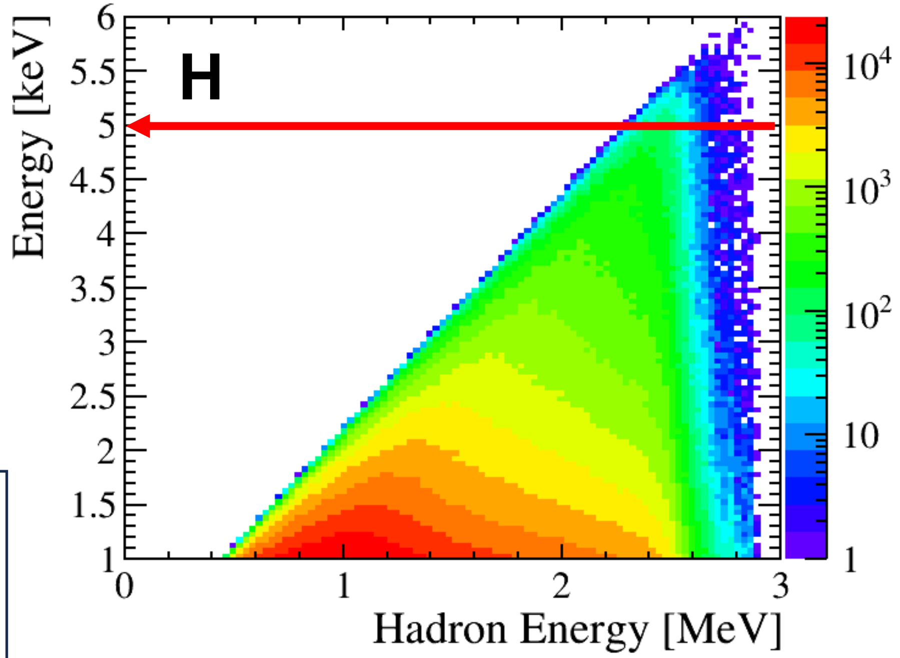

Only H has the **δ electron >** 5 keV.

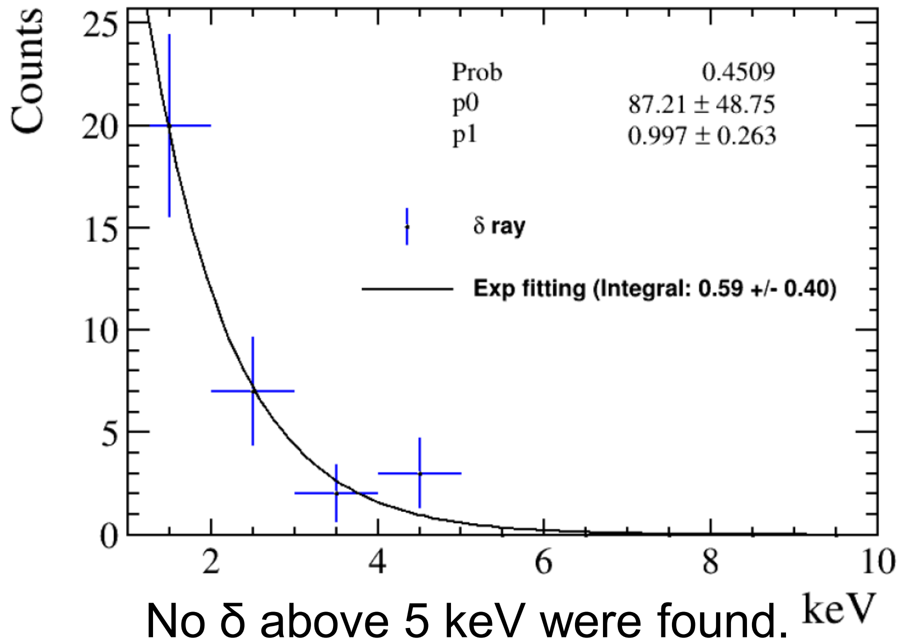

No δ above 5 keV were found.

Estimate by extrapolating from the exponential fit

- Consider the selection efficiency for δ-electrons.
- **Finally get: 0.035±0.023(stat.)**

2. 偶然符合本底

- **Method 2: 数据驱动的方法**
  - 选取实验数据中的核径迹控制样本与光电子径迹在同一帧上的事例.
  - 考虑偶然符合在统一顶点的几率,得到最终本底结果为： **0.180±0.022(stat.)±0.042(sys.)**

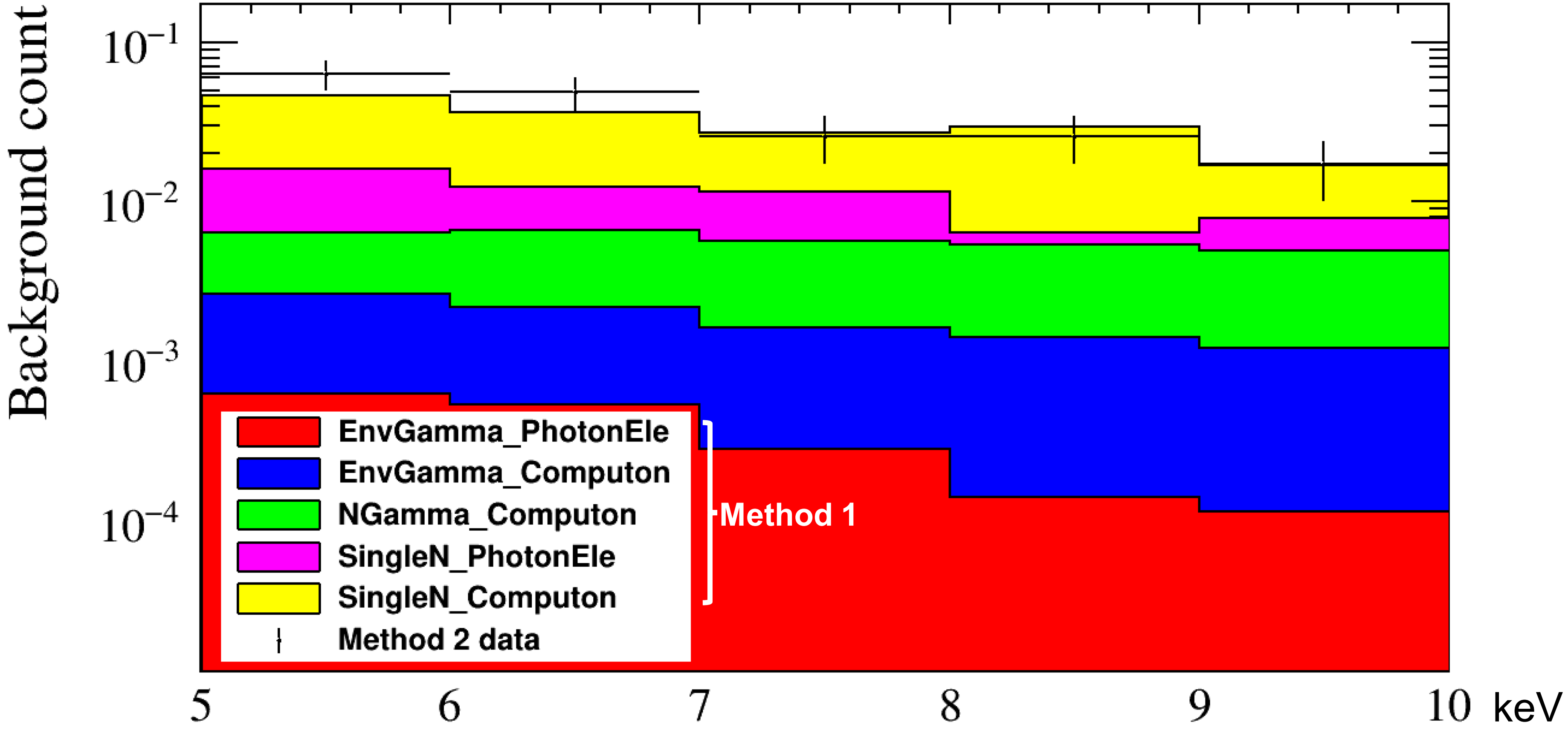

方法一与方法二的结果在统计误差范围内一致。

相对截面计算

- Migdal过程截面与核反冲截面的比值:

$$P_{\mathrm{Migdal}}(5\mathrm{keV}<\mathrm{ER}<10\mathrm{keV},\ \mathrm{NR}>35\mathrm{keVee})=\frac{\left(\frac{n_{\mathrm{obs}}^{\mathrm{ER}}-n_{\mathrm{obs}}^{\mathrm{bg}}}{\varepsilon_{\mathrm{acc}}\varepsilon_{\mathrm{NR}}\varepsilon_{\mathrm{ER}}}\right)}{\left(\frac{n_{\mathrm{tot}}^{\mathrm{NR}}}{\varepsilon_{\mathrm{acc}}\varepsilon_{\mathrm{NR}}}\right)}=\frac{(n_{\mathrm{obs}}^{\mathrm{ER}}-n_{\mathrm{obs}}^{\mathrm{bg}})}{\varepsilon_{\mathrm{ER}}n_{\mathrm{tot}}^{\mathrm{NR}}}$$

- 参数:

	Efficiency/Count	Statistical Error	Systematic Error
Efficiency $\varepsilon_{\mathrm{ER}}$	14.4% 29%(YOLO)*49%(vertx rec)	±0.1%	±1.9%
$n_{\mathrm{tot}}^{\mathrm{NR}}$	8.17×10^5	±903	±35880
$n_{\mathrm{obs}}^{\mathrm{ER}}$	6	±2.449	
$n_{\mathrm{obs}}^{\mathrm{bg}}$	0.229	±0.032	±0.043

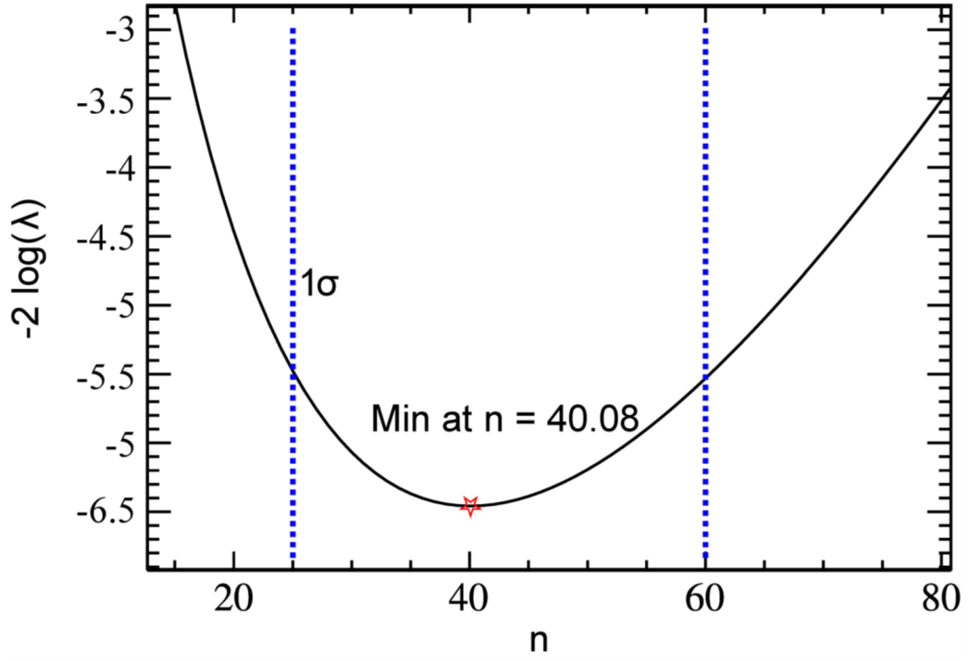

- 上下限的计算方式: $$\Delta P_{\pm}=\sqrt{\left(\frac{n_{min}-n_{ul/ll}}{n_{min}}\right)^2+\left(\frac{n_{\mathrm{tot\,error}}^{\mathrm{NR}}}{n_{\mathrm{tot}}^{\mathrm{NR}}}\right)^2}\cdot\frac{n_{min}}{n_{\mathrm{tot}}^{\mathrm{NR}}}$$

最终结果: $4.91^{+2.56}_{-1.87}\times10^{-5}$

总跃迁几率

$$\sum_{nl} \frac{dp^i(nl \to E_e)}{dE_e}$$

初态为 (n, l) 的电子跃迁到具有 E_e 能量末态的几率.

武雷

祝斌

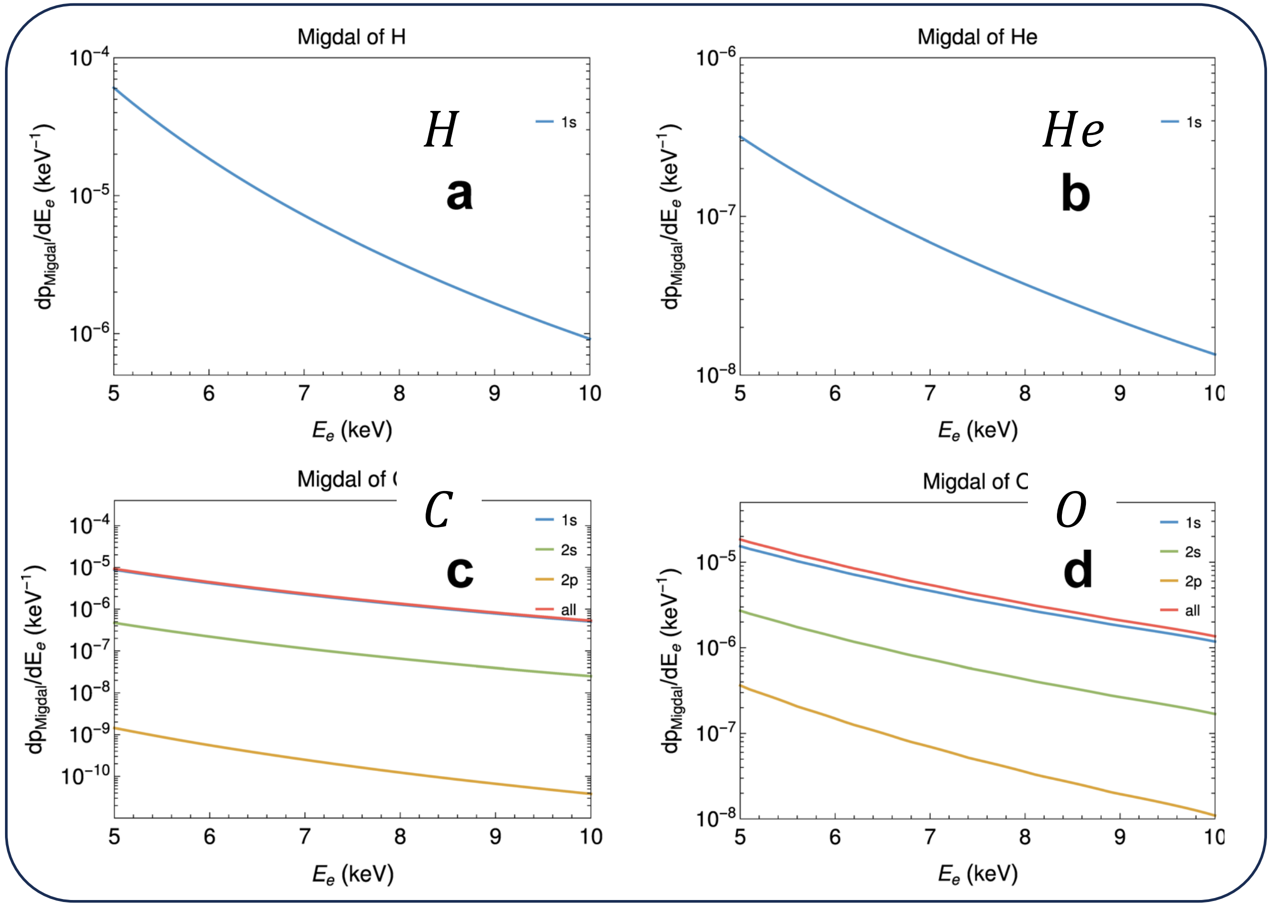

每种元素的跃迁几率

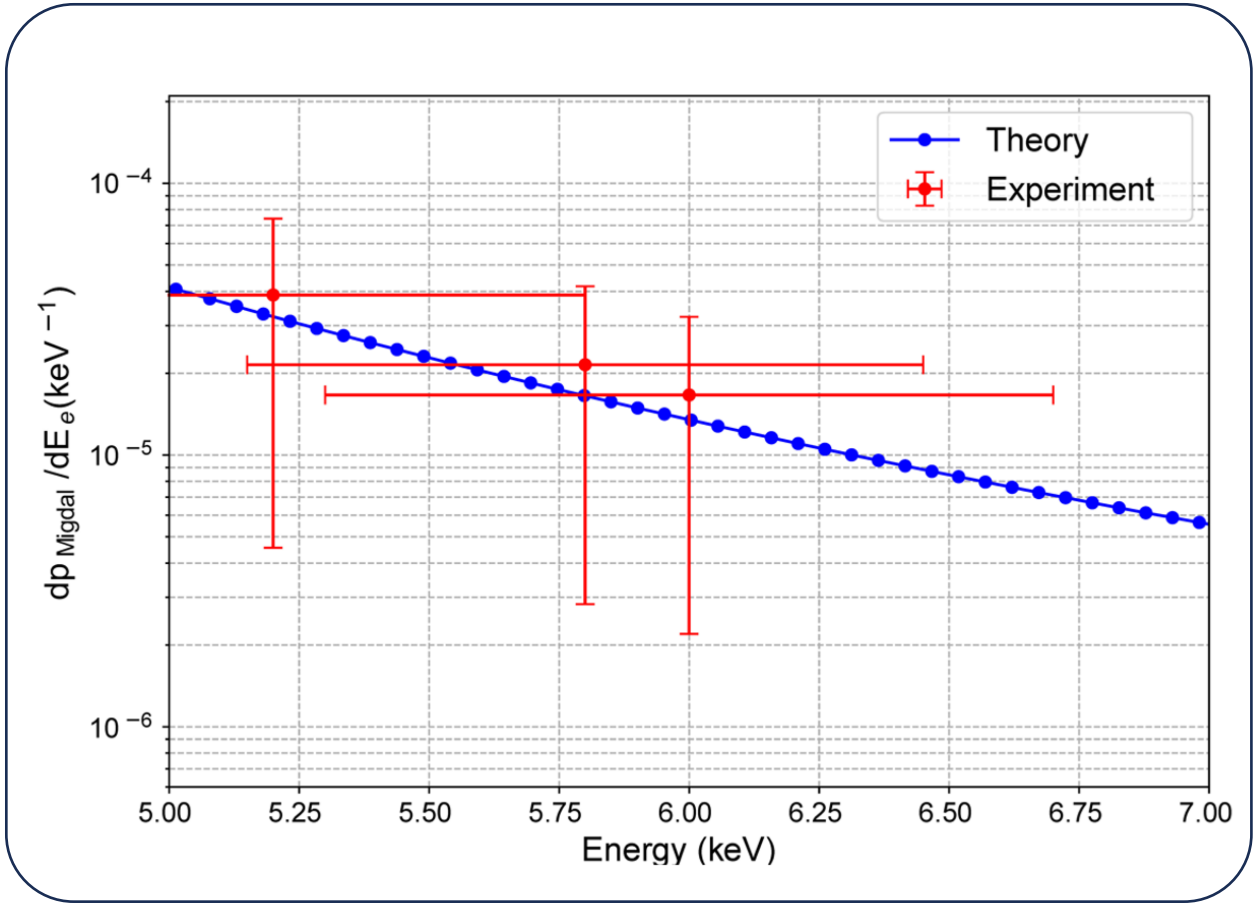

总跃迁几率

Upgrade in progress

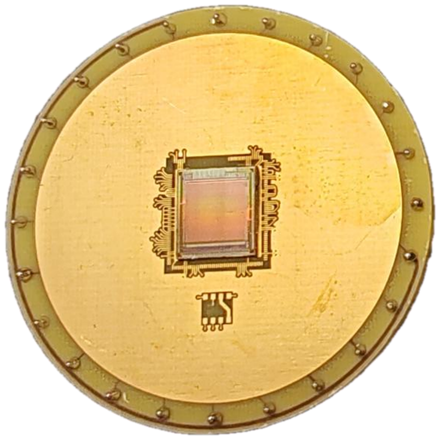

Topmetal-II

Topmetal-L

	Topmetal-II$^-$	Topmetal-L
Chip size [mm^2]	8×9	17×24
Active area [mm^2]	6×6	16.02×23.04
Pixel array	72×72	356×512
Pixel density [pixels/mm^2]	145	494
Power density [W/cm^2]	2.778	0.195
Pixel gain [μV/e$^-$]	-	76.04
ENC [e$^-$]	13.9	22.8
Readout mode	Rolling Shutter	Rolling Shutter / Sentinel
Time cost	2.6 ms/frame	0.73 ms/frame @ Sentinel

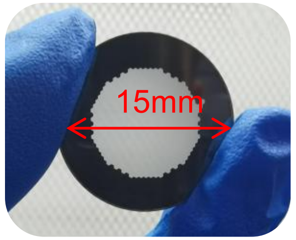

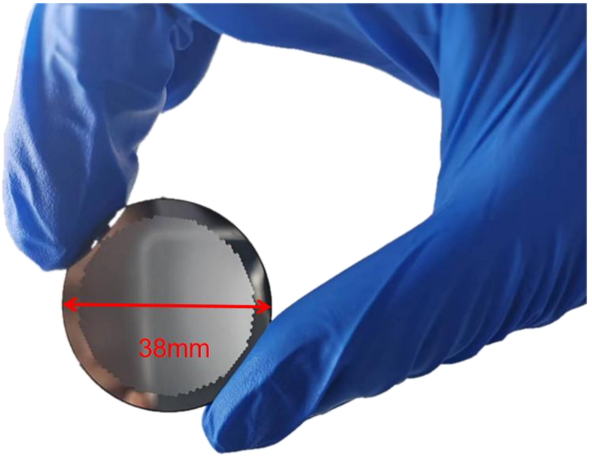

Larger GMCP

- 6x6 mm, 83 um in pitch -> 2.3x1.5 cm, 45 um in pitch
- Fresh time: 2.6 ms/Frame -> 0.7 ms/Frame
- Readout logic: Rolling Shutter -> Sensitive area

Upgrade in progress

Sensitive area readout:

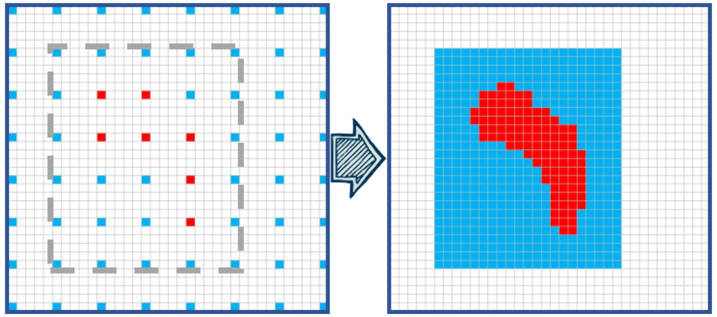

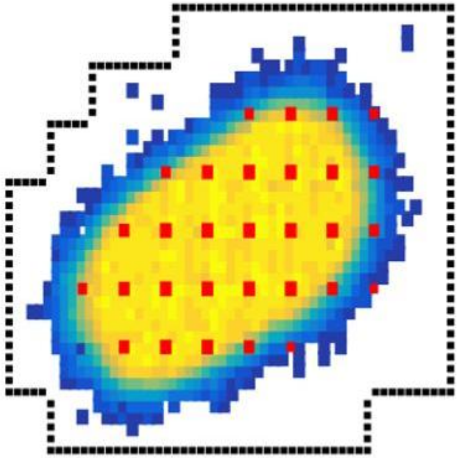

Sensitive pixels

Readout pixels range

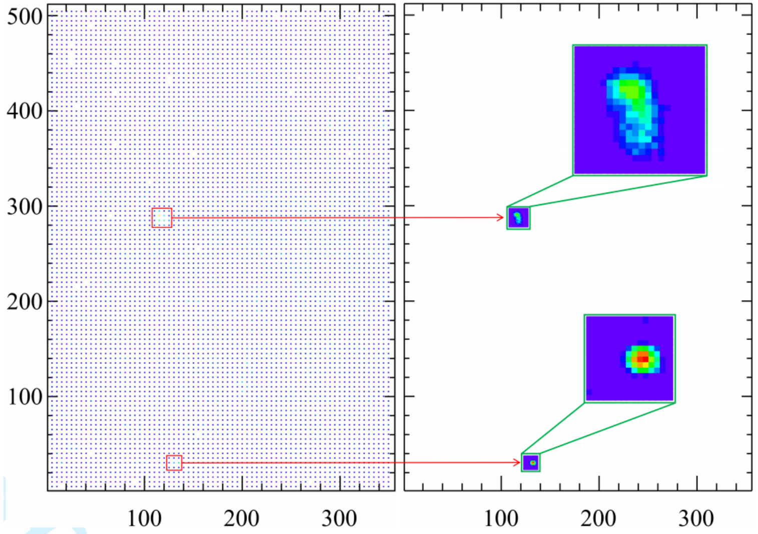

arXiv:2511.15130

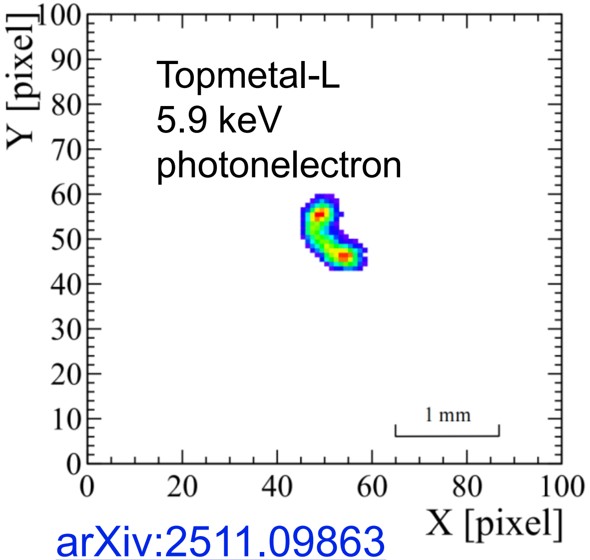

arXiv:2511.09863

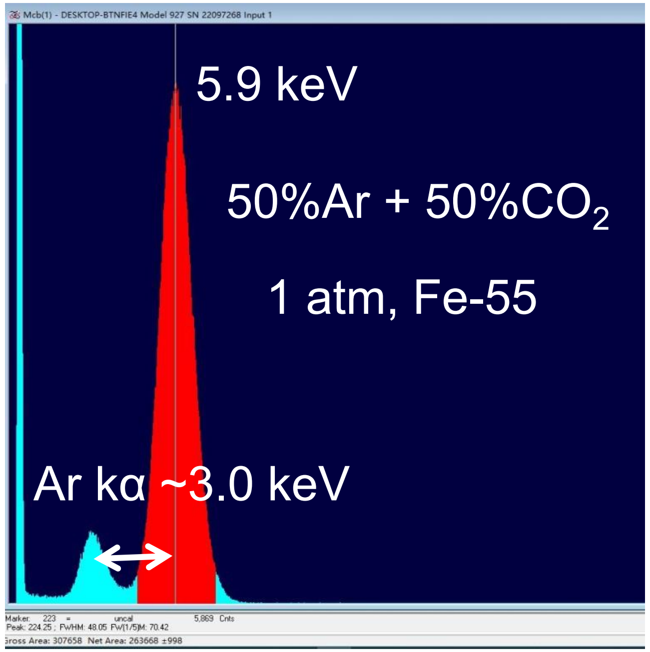

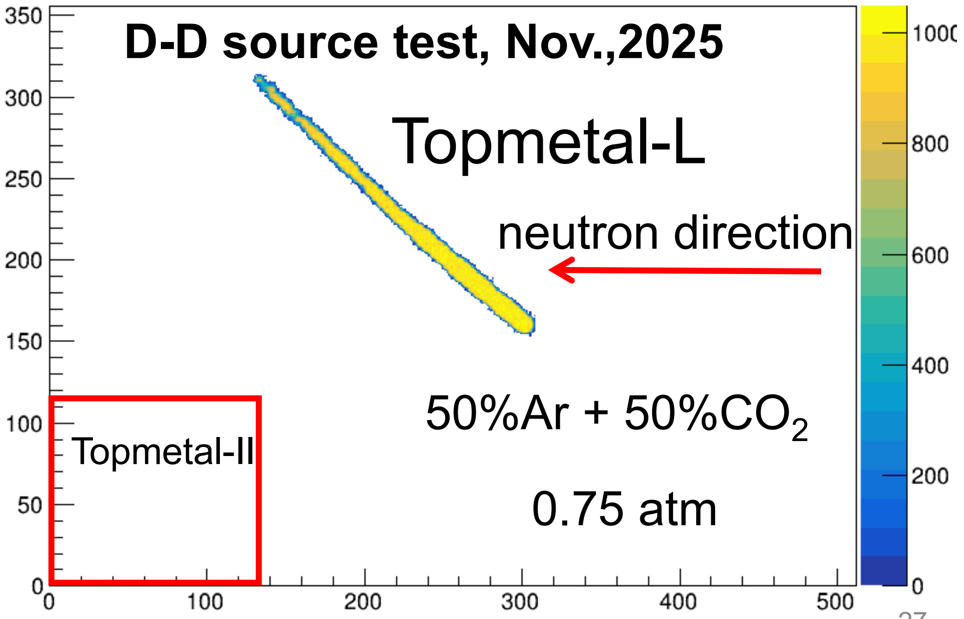

总结

- 首次直接证实了1939年利用量子力学预言的Migdal效应，也为轻暗物质探测突破阈值瓶颈提供了关键支撑。

- 下一步计划：
  - 升级实验装置，提高统计量，提升Migdal截面测量精度
  - 测量常见暗物质探测核素的Migdal截面
  - 测量Migdal截面的能量依赖

谢 谢！